Int J Gynecol Cancer 2008, **18**, 908–912

Primary retroperitoneal mucinous cystadenocarcinoma associated with pregnancy

K. KASHIMA, T. YAHATA, K. FUJITA & K. TANAKA
Division of Obstetrics and Gynecology, Department of Cellular Function, Niigata University, Graduate School of Medical and Dental Sciences, Niigata, Japan

Abstract. Kashima K, Yahata T, Fujita K, Tanaka K. Primary retroperitoneal mucinous cystadenocarcinoma associated with pregnancy. *Int J Gynecol Cancer* 2008;**18**:908–912.

Primary retroperitoneal mucinous cystadenocarcinoma (PRMC) is an extremely rare tumor. Only 30 cases have been reported previously in the English literature, and little information is available concerning its treatment and prognosis. The patient was a 28-year-old woman, presenting with a right mid-abdominal tumor at 26 weeks of gestation. At 31 weeks of gestation, she underwent an exploratory laparotomy and was diagnosed with a PRMC. No disseminated tumor was observed, and an excision of only the tumor was performed. She had an uneventful vaginal delivery at 38 weeks of gestation and remains free of disease at 13 months after the operation. This report describes a case of PRMC associated with pregnancy. The optimal management of these retroperitoneal masses during pregnancy is discussed. Based on limited experience and the current literature, a PRMC with an intact capsule and no dissemination appears to have a good prognosis and can be treated by tumor excision alone in patients who wish to preserve fertility.

KEYWORDS: conservative surgery, pregnancy, retroperitoneal mucinous cystadenocarcinoma.

Primary retroperitoneal mucinous cystadenocarcinoma (PRMC) and its counterpart of borderline malignancy remain extremely rare, with few reported cases in the English literature[1–26]. Most of the reported patients were female[4,26]. The incidence of these tumors is higher in premenopausal women than in postmenopausal women. Although these tumors resemble ovarian mucinous cystic neoplasms, there is no consensus on the standard treatment due to their low frequency. The majority of reported PRMC cases were treated with radical surgery, which included extirpation of the tumor together with a total hysterectomy and a bilateral salpingo-oophorectomy, with good prognosis. On the other hand, more conservative surgery is performed in reproductive-aged women who wish to preserve their fertility. The present article reports the first case of a PRMC treated by fertility-sparing surgery during pregnancy, with a good perinatal outcome.

Address correspondence and reprint requests to: Tetsuro Yahata, MD, PhD, Division of Obstetrics and Gynecology, Department of Cellular Function, Niigata University, Graduate School of Medical and Dental Sciences, 1-757 Asahimachi-dori, Niigata 951-8510, Japan. Email: yahatat@med.niigata-u.ac.jp

doi:10.1111/j.1525-1438.2007.01130.x

Case report

A 28-year-old, gravida 2, para 2 woman was referred to this hospital because of a large tumor in the right mid-abdomen, found by a routine ultrasound examination at 28 weeks of gestation. An ultrasound examination demonstrated a single normally grown fetus and regular amniotic fluid volume, and the patient was asymptomatic. Magnetic resonance imaging showed a retroperitoneal, 17-cm, multicystic tumor containing a solid component without invasive infiltration of the adjacent abdominal organs (Fig. 1). No ascites was detected. Routine ultrasound examinations at 12 and 20 weeks of gestation showed no abnormalities. Tumor markers, including CA125, CA19-9, and carcinoembryonic antigen, were all within the normal limits.

An exploratory laparotomy was performed at 31 weeks of gestation. A well-encapsulated retroperitoneal mass of about 17 cm diameter was found, lying adjacent to the caudal pole of the left kidney. The ovaries, fallopian tubes, appendix, colon, and kidneys all

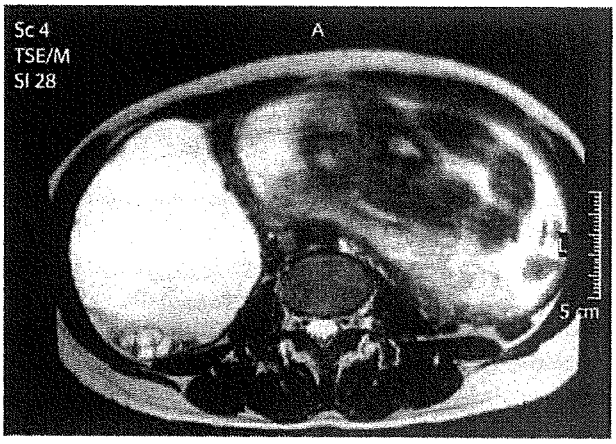

Figure 1. Magnetic resonance imaging demonstrated a cystic tumor containing a solid component (T2-weighted magnetic resonance image).

appeared normal without intraperitoneal implants or ascites. The abdominal washing cytology was negative for malignant cells. The tumor was not connected to surrounding organs, and it was easily removed without rupture of the capsule.

Macroscopically, the tumor showed a large multilocular cyst filled with mucinous fluid. The external surface was smooth. Foci of papillary projecting lesions measuring up to 0.5 cm were found over the inner surface. Pathologic examinations revealed a well-differentiated mucinous cystadenocarcinoma (Fig. 2). Neither penetration nor infiltration of the external surface could be detected, and no separate ovarian tissue was found.

The postoperative recovery was uneventful, and she was discharged from the hospital at 34 weeks of gestation. She was followed up for her pregnancy in this hospital as an outpatient with an uneventful course. A normal vaginal delivery occurred at 38 weeks and 6 days of gestation, and the infant was a normal healthy 2744-g female. Computed tomographic scans of the chest, abdomen, and pelvis revealed no evidence of disease and no other possible intra- and extraabdominal sites of tumor origin. No adjuvant therapy was administered. She has been regularly followed up at the hospital and is presently doing well without any recurrence 13 months after the surgery.

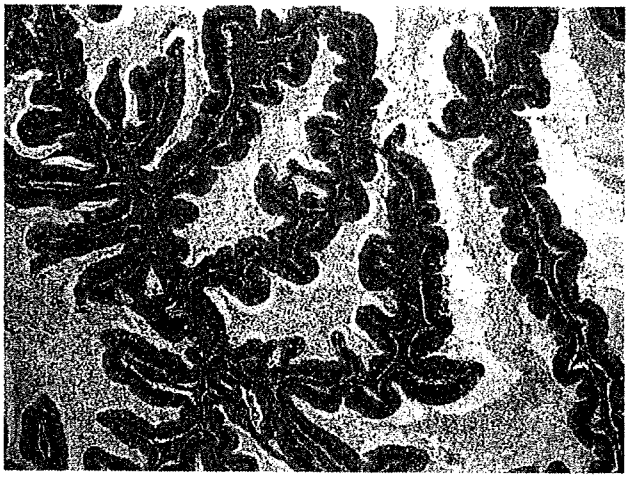

Figure 2. Microscopic examinations showed a mucinous cystadenocarcinoma (hematoxylin and eosin stain at ×100).

Discussion

PRMC is an extremely rare condition, with approximately 30 cases described in the English literature. The mean age was 43.3 years, with a range from 17 to 86 years. Forty-five percent of patients were in their reproductive age (16–40 years), and fertility preservation is an important issue in the management of this tumor. There has been only one reported case of PRMC associated with pregnancy, and this is the first patient with a PRMC who was treated by conservative surgery during pregnancy, with a good perinatal outcome.

Although minimal data are available concerning the treatment of PRMC, it has been treated the same as a primary ovarian mucinous carcinoma of the comparable stage[5,15,17]. However, unlike ovarian carcinomas, no standard treatment exists for retroperitoneal neoplasms because little is known concerning the optimal treatment and prognosis of PRMC or its borderline tumor due to its rarity. In patients with a mucinous retroperitoneal tumor of borderline malignancy, only tumor excision was performed in all but one case (Table 1). A paraovarian recurrence 21 months later was reported in only one of those cases[1], and therefore, tumor resection alone may be acceptable for borderline malignant tumors. Most of the follow-up results in patients with PRMC were excellent (Table 2). Three cases died at 4, 6, and 18 months after the initial surgery with an excision of the tumor alone[11,16,23]. Two of them had extracystic extensions, capsule invasion in one patient and tumor rapture in the other patient. Some authors have noted that the removal of both the ovaries and the uterus, in addition to an excision of the retroperitoneal tumor, should be performed to improve the prognosis after surgery, even though the ovaries and the uterus appear to be normal[16,19,22]. On the other hand, long-term survival of more than 5 years has been reported in the cases treated with only tumor excision[20,25]. Therefore, an excision of the mass alone should be considered for young women who wish to preserve their fertility, provided the tumor remains confined to the retroperitoneum,

Table 1. Cases of primary retroperitoneal mucinous tumor of borderline malignancy reported in the literature

Reference	Age (years)	Sex	Size (cm)	Tumor marker	Extracystic extension	Treatment	Adjuvant treatment	Outcome after surgery (months)
Storch and Raghavan[1]	17	Female	17	Unknown	No	TE	Cx (Cytoxan)	Paraovarian recurrence (21)
Banerjee and Gough[2]	47	Female	13	Unknown	No	TE + splenectomy + left adrenalectomy	No	Unknown
Soundergaard and Kaspersen[3]	37	Female	18	Unknown	No	TE + RH	Omentectomy + Appe.	NED (18)
Motoyama *et al.*[4]	42	Male	6	Unknown	Needle aspiration	TE	Unknown	Unknown
Pearl *et al.*[5]	33	Female	33	Normal	Needle aspiration	TE (laparoscopy)	No	NED (10)
Papadogiannakis *et al.*[6]	33	Female	15	Unknown	No	TE	No	NED (12)
Chen *et al.*[7]	48	Female	15	Unknown	Needle aspiration	TE (laparoscopy)	No	NED (8)
Kessler *et al.*[8]	38	Female	11.5	Normal	Needle aspiration	TE + resection of descending colon + Appe.	No	NED (60)
Gutsu *et al.*[9]	41	Female	21	Unknown	No	TE	No	NED (18)
Matsubara *et al.*[10]	36	Female	12	CA125, CA19-9	No	TE + Appe.	No	NED (6)

TE, tumor excision; RH, radical hysterectomy; Appe., appendectomy; Cx, chemotherapy; NED, no evidence of disease.

with well-to-moderate differentiation and no evidence of any tumor spread.

The management of ovarian tumors during pregnancy can be challenging for both the patient and the clinician. Most ovarian tumors diagnosed during pregnancy are relatively small functional cyst, so these tumors can and should be managed conservatively. The incidence of ovarian malignancy detected during pregnancy is very low, 1/10,000 to 1/50,000 pregnancies, in most reports[27,28]. If malignancy is suggested for the tumor, then prompt treatment of the mother is necessary. Presently, surgery with adequate staging remains the cornerstone of ovarian cancer therapy during pregnancy. When a malignancy is present during pregnancy, typically germ cell and borderline ovarian tumors are observed[27]. For patients with these good risk tumors who wish to preserve fertility, conservative surgery can be considered. Even if the tumor is invasive, fertility-sparing surgery could be considered for the patients with apparent early disease such as stage IA or IC invasive ovarian cancers. The consequences of the conservative treatment for the mother and infant are quite favorable. Prognosis for epithelial ovarian cancer diagnosed during pregnancy is similar to that of nonpregnant women[29]. However, increased risks of blood transfusions, cesarean section, hysterectomy, and prolonged hospitalization for the mother and increased risks of prematurity and very low-birthweight infants associated with the surgical intervention for an ovarian tumor during pregnancy have been reported[30].

There has been only one reported case of PRMC associated with pregnancy[24]. The patient presented with a cystic tumor in the left upper abdomen at 30 weeks of pregnancy. She was managed conservatively during pregnancy. The tumor was removed with an intact capsule following an elective cesarean section at 38 weeks of pregnancy, and she remained disease free 1 year after the surgery. Since malignancy was suspected in the current case, conservative surgery was thus performed during pregnancy. Following tumor removal, she continued to carry the baby to full term.

Although this neoplasm has been recommended to be treated like an analogous primary ovarian cancer, the advantages of adjuvant chemotherapy have not yet been proven. Patients may benefit from chemotherapy if the cyst ruptures or dissemination is observed. In the present case, the tumor was completely resected with an intact capsule, and adjuvant chemotherapy was not planned either during pregnancy or after the delivery. The patient has shown no evidence of recurrence for 13 months after the surgery.

Based on the limited experience of the authors and according to a survey of the pertinent literature, a

Table 2. Cases of PRMC reported in the literature

Reference	Age (years)	Sex	Size (cm)	Tumor marker	Extracystic extension	Treatment	Adjuvant treatment	Outcome after surgery (months)
Roth and Ehrlich[11]	48	Female	Unknown	Unknown	No	TE	No	DOD (6)
Fujii *et al.*[12]	69	Female	23	Normal	No	TE + TAH + BSO	No	NED (36)
Nelson *et al.*[13]	35	Female	20	Normal	No	TE	TAH + BSO	NED (22)
Jorgensen and Vibits[14]	38	Female	8	Unknown	No	TE	No	NED (9)
Park *et al.*[15]	40	Female	24	Normal	No	TE	TAH + BSO + biopsy of omentum	NED (3)
Gotoh *et al.*[16]	44	Female	12.5	CA125	Capsule invasion	TE × Cx (tegaful-uracil)	Cx (CDDP + mitomycin C)	DOD (4)
Motoyama *et al.*[4]	42	Female	11	Unknown	Needle aspiration	TE	Unknown	Unknown
Tenti *et al.*[17]	46	Female	20	CA125, AFP	Rupture	TE	TAH + BSO × Cx (CDDP + CPM)	NED (33)
Tenti *et al.*[17]	45	Female	20	Unknown	No	TE	TAH + BSO + PLN + omentectomy	NED (19)
Carabias *et al.*[18]	43	Female	15	Unknown	No	TE + cholecystectomy + Appe.	TAH + BSO	NED (24)
Lee *et al.*[19]	55	Female	20	Normal	No	TE	TAH + BSO + PLN + omentectomy	NED (30)
Lee *et al.*[19]	45	Female	17	Normal	No	TE + TAH + BSO	No	NED (15)
Uematsu *et al.*[20]	86	Female	23	CEA	Peritoneal implant	TE + gastrectomy	No	NED (72)
Suzuki *et al.*[21]	40	Female	15	CA19-9	No	TE + partial ileocecum resection + Appe.	No	NED (15)
Tangjitgamol *et al.*[22]	41	Female	12	Unknown	No	TE + TAH + BSO + Appe.	Cx (CDDP + CPM)	NED (18)
Mikami *et al.*[23]	38	Female	16	Normal	Rupture	TE × Cx (CDDP + ADM + CPM)	Tumor nodule excision + PLN + PAN	DOD (18)
Sonntag *et al.*[24]	30	Female	5	CA19-9	No	TE + cesarean section	No	NED (12)
Law *et al.*[25]	35	Female	11	Normal	No	TE	No	NED (60)
Thamboo *et al.*[26]	64	Male	24	Unknown	No	TE	No	NED (18)
Present case	28	Female	17	Normal	No	TE	No	NED (10)

TE, tumor excision; TAH, total abdominal hysterectomy; BSO, bilateral salpingo-oophorectomy; PLN, pelvic lymphadenectomy; PAN, para-aortic lymphadenectomy; Appe., appendectomy; Cx, chemotherapy; CDDP, cisplatin; CPM, cyclophosphamide; ADM, adriamycin; NED, no evidence of disease; DOD, died of disease; AFP, alpha-fetoprotein; CEA, carcinoembryonic antigen.

PRMC that has an intact capsule and no dissemination appears to have a good prognosis and may therefore be treated by tumor excision alone in young patients who wish to preserve their fertility. However, thorough examinations of the pelvis as well as the abdominal organs are necessary to determine both the possibility of tumor invasion and the primary origin of the lesion.

References

1 Storch MP, Raghavan U. Mucinous cystadenocarcinoma of retroperitoneum. *Conn Med* 1980;**44**:140–1.
2 Banerjee R, Gough J. Cystic mucinous tumours of the mesentery and retroperitoneum: report of three cases. *Histopathology* 1988;**12**:527–32.
3 Sondergaard G, Kaspersen P. Ovarian and extraovarian mucinous tumors with solid mural nodules. *Int J Gynecol Pathol* 1991;**10**:145–55.
4 Motoyama T, Chida T, Fujiwara T, Watanabe H. Mucinous cystic tumor of the retroperitoneum. A report of two cases. *Acta Cytol* 1994;**38**:261–6.
5 Pearl ML, Valea F, Chumas J, Chalas E. Primary retroperitoneal mucinous cystadenocarcinoma of low malignant potential: a case report and literature review. *Gynecol Oncol* 1996;**61**:150–2.
6 Papadogiannakis N, Gad A, Ehliar B. Primary retroperitoneal mucinous tumor of low malignant potential: histogenetic aspects and review of the literature. *APMIS* 1997;**105**:483–6.
7 Chen JS, Lee WJ, Chang YJ, Wu MZ, Chiu KM. Laparoscopic resection of a primary retroperitoneal mucinous cystadenoma: report of a case. *Surg Today* 1998;**28**:343–5.
8 Kessler TM, Kessler W, Neuweiler J, Nachbur BH. Treatment of a case of primary retroperitoneal mucinous cystadenocarcinoma: is adjuvant hysterectomy and bilateral salpingo-oophorectomy justified? *Am J Obstet Gynecol* 2002;**187**:227–32.
9 Gutsu E, Mishin I, Gagauz I. Primary retroperitoneal mucinous cystadenoma. A case report and brief review of the literature. *Zentralbl Chir* 2003;**128**:691–3.
10 Matsubara M, Shiozawa T, Tachibana R *et al.* Primary retroperitoneal mucinous cystadenoma of borderline malignancy: a case report and review of the literature. *Int J Gynecol Pathol* 2005;**24**:218–23.
11 Roth LM, Ehrlich CE. Mucinous cystadenocarcinoma of the retroperitoneum. *Obstet Gynecol* 1977;**49**:486–8.
12 Fujii S, Konishi I, Okamura H, Mori T. Mucinous cystadenocarcinoma of the retroperitoneum: a light and electron microscopic study. *Gynecol Oncol* 1986;**24**:103–12.
13 Nelson H, Benjamin B, Alberty R. Primary retroperitoneal mucinous cystadenocarcinoma. *Cancer* 1988;**61**:2117–21.
14 Jorgensen LJ, Vibits H. Primary retroperitoneal mucinous cystadenocarcinoma. A case report and review of the literature. *APMIS* 1991;**99**:1055–7.
15 Park U, Han KC, Chang HK, Huh MH. A primary mucinous cystoadenocarcinoma of the retroperitoneum. *Gynecol Oncol* 1991;**42**:64–7.
16 Gotoh K, Konaga E, Arata A, Takeuchi H, Mano S. A case of primary retroperitoneal mucinous cystadenocarcinoma. *Acta Med Okayama* 1992;**46**:49–52.
17 Tenti P, Carnevali L, Tateo S, Durola R. Primary mucinous cystoadenocarcinoma of the retroperitoneum: two cases. *Gynecol Oncol* 1994;**55**:308–12.
18 Carabias E, Garcia Munoz H, Dihmes FP, Lopez Pino MA, Ballestin C. Primary mucinous cystadenocarcinoma of the retroperitoneum. Report of a case and literature review. *Virchows Arch* 1995;**426**:641–5.
19 Lee IW, Ching KC, Pang M, Ho TH. Two cases of primary retroperitoneal mucinous cystadenocarcinoma. *Gynecol Oncol* 1996;**63**:145–50.
20 Uematsu T, Kitamura H, Iwase M *et al.* Ruptured retroperitoneal mucinous cystadenocarcinoma with synchronous gastric carcinoma and a long postoperative survival: case report. *J Surg Oncol* 2000;**73**:26–30.
21 Suzuki S, Mishina T, Ishizuka D, Fukase M, Matsubara YI. Mucinous cystadenocarcinoma of the retroperitoneum: report of a case. *Surg Today* 2001;**31**:747–50.
22 Tangjitgamol S, Manusirivithaya S, Sheanakul C, Leelahakorn S, Thawaramara T, Kaewpila N. Retroperitoneal mucinous cystadenocarcinoma: a case report and review of literature. *Int J Gynecol Cancer* 2002;**12**:403–8.
23 Mikami M, Tei C, Takehara K, Komiyama S, Suzuki A, Hirose T. Retroperitoneal primary mucinous adenocarcinoma with a mural nodule of anaplastic tumor: a case report and literature review. *Int J Gynecol Pathol* 2003;**22**:205–8.
24 Sonntag B, Lelle RJ, Steinhard J, Brinkmann OA, Hungermann D, Kiesel L. Retroperitoneal mucinous adenocarcinoma occuring during pregnancy in a supernumerary ovary. *J Obstet Gynaecol* 2005;**25**:515–6.
25 Law KS, Chang TM, Tung JN. Fertility-sparing treatment of a primary retroperitoneal mucinous cystadenocarcinoma. *BJOG* 2006;**113**:612–4.
26 Thamboo TP, Sim R, Tan SY, Yap WM. Primary retroperitoneal mucinous cystadenocarcinoma in a male patient. *J Clin Pathol* 2006;**59**:655–7.
27 Dgani R, Shoham Z, Atar E, Zosmer A, Lancet M. Ovarian carcinoma during pregnancy: a study of 23 cases in Israel between the years 1960 and 1984. *Gynecol Oncol* 1989;**33**:326–31.
28 Ferrandina G, Distefano M, Testa A, De Vincenzo R, Scambia G. Management of an advanced ovarian cancer at 15 weeks of gestation: case report and literature review. *Gynecol Oncol* 2005;**97**:693–6.
29 Machado F, Vegas C, Leon J *et al.* Ovarian cancer during pregnancy: analysis of 15 cases. *Gynecol Oncol* 2007;**105**:446–50.
30 Leiserowitz GS, Xing G, Cress R, Brahmbhatt B, Dalrymple JL, Smith LH. Adnexal masses in pregnancy: how often are they malignant? *BJOG* 2006;**101**:315–21.

Accepted for publication June 19, 2007

doi:10.1111/j.1447-0756.2009.01054.x J. Obstet. Gynaecol. Res. Vol. 35, No. 5: 1000–1003, October 2009

Extranodal Rosai–Dorfman disease involving bilateral ovaries in a patient with a ventriculoperitoneal shunt

Masayuki Yamaguchi[1], Tetsuro Yahata[1], Kazuyuki Fujita[1], Junko Sakurada[2], Go Hasegawa[2], Hajime Umezu[2], Makoto Naito[2] and Kenichi Tanaka[1]

Departments of [1]Obstetrics and Gynecology and [2]Cellular and Molecular Pathology, Niigata University Graduate School of Medical and Dental Sciences, Niigata City, Niigata, Japan

Abstract

Rosai–Dorfman disease (RDD) is a rare condition of unknown etiology, and female genital tract involvement in RDD is uncommon. We describe the first case of RDD with bilateral ovarian involvement in a patient implanted with a ventriculoperitoneal (VP) shunt. The patient was a 17-year-old Japanese woman who had undergone radiotherapy, surgery for extranodal RDD involving the brain, and VP shunt insertion at age 12. Bilateral pelvic masses were incidentally detected on a computed tomography scan. She underwent laparotomy for lesion extirpation. On abdominal washing cytology, histiocytes showing emperipolesis were identified. Bilateral salpingo-oophorectomy was performed instead of extirpation, as it was difficult to identify the lesion margins. At 24 months after surgery, the patient is well and has not developed local recurrence. Thus, RDD can recur because of implantation of lesion cells into the abdominal cavity through a VP shunt, as is observed in the case of cerebral neoplasms.

Key words: ovarian mass, Rosai–Dorfman disease, VP shunt.

Introduction

Rosai–Dorfman disease (RDD) or sinus histiocytosis with massive lymphadenopathy was first described by Rosai and Dorfman in 1969.[1] It is characterized by massive painless cervical lymphadenopathy, low-grade fever, leukocytosis, increased erythrocyte-sedimentation rate, and polyclonal hypergammaglobulinemia. The mean age at onset is reported to be 20.6 years with a male : female incidence ratio of 1.4:1.[2] Extranodal involvement is present in approximately 43% of cases, and the commonly involved sites are the skin, upper respiratory tract, bone, orbit, paranasal sinuses, the central nervous system (CNS) etc.[3] Involvement of the female genital tract is extremely rare, with only one reported case of uterine cervical involvement.[4] Microscopic features of the involved lymph nodes are perinodal fibrosis and expanded sinuses with non-neoplastic proliferation of histiocytes. These histiocytes are immunoreactive for S-100 protein, CD14, CD68, and vimentin but negative for CD1a. Lymphocytophagocytosis or emperipolesis is a characteristic finding of the disease.

The etiology, pathogenesis, and natural history of RDD are unknown. At present, this condition is considered as a benign or reactive proliferation that undergoes spontaneous regression. In contrast, extranodal RDD often mimics a malignant tumor.[5] Patients may develop recurrence or progressive disease, and multi-organ involvement has been reported. We discuss the first case of a young female patient with a history of intracranial RDD who presented with ovarian involvement, possibly associated with a ventriculoperitoneal (VP) shunt placed at the time of

Received: August 27 2008.
Accepted: December 19 2008.
Reprint request to: Dr Tetsuro Yahata, Department of Obstetrics and Gynecology, Niigata University Graduate School of Medical and Dental Sciences, 1-757, Asahimachi-dori, Chuo Ward, Niigata City, Niigata 951-8510, Japan. Email: yahatat@med.niigata-u.ac.jp

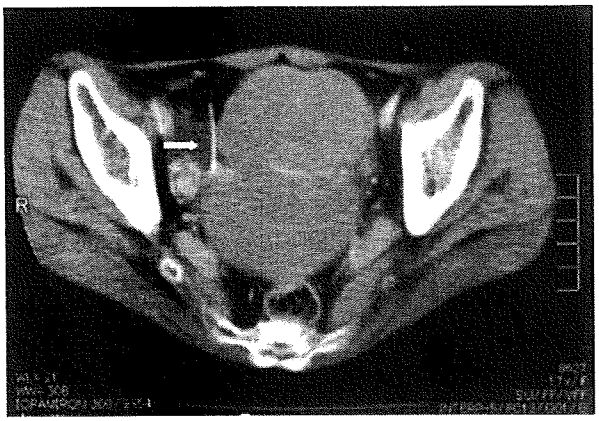

Figure 1 A computed tomography scan showing pelvic masses. The ventriculoperitoneal shunt is indicated by an arrow.

resection of the primary meningeal lesion 5 years previously.

Case Report

The patient was a 17-year-old Japanese woman with a history of radiation therapy and surgical resection of a primary meningeal lesion and VP shunt insertion at the age of 12. The results of pathological examination of the tumor led to a diagnosis of RDD. The patient was administered additional radiation therapy for multiple recurrent lesions in the spinal cord at ages 13 and 16. She had been doing well until February 2006, when she presented to a hospital with a slight fever and general fatigue. Hematological examination revealed elevation of the C-reactive protein (CRP) level (13.3 mg/dL) without leukocytosis. Meningitis was suspected, but an examination of the cerebrospinal fluid disclosed no abnormality. Despite the administration of panipenem/betamipron, the CRP level remained elevated. In order to identify the infectious focus, a systemic computed tomography (CT) scan was obtained, and incidental pelvic masses were observed in close proximity to the VP shunt catheter (Fig. 1).

Subsequently, the patient was referred to our hospital for further evaluation and treatment of the pelvic masses. At the first visit to our hospital, she complained of abdominal distension and polyuria. On pelvic examination, bilateral mobile pelvic masses were noted, and a magnetic resonance (MR) image showed 7- and 8-cm-wide solid masses that were located side-by-side, were well demarcated, and had smooth surfaces. The intensity of the masses was low on T1-weighted MR images and intermediate on T2-weighted MR images; the masses were well enhanced on contrast-enhanced MR images (Fig. 2). The levels of tumor markers such as carcinoembryonic antigen, CA-125, CA19-9, and alpha-fetoprotein were all within normal limits. The radiological differential diagnoses, determined on the basis of the finding of solid and well-demarcated masses, were fibroma, thecoma, leiomyoma etc. A diagnosis of extranodal RDD with bilateral ovarian involvement was made because the masses were similar to the previous meningeal lesion, particularly with regard to the signal intensities on MR imaging. Laparotomy for the extirpation of the lesion with preservation of the normal ovarian tissue was planned. Intraoperative exploration revealed solid, mobile, bilateral ovarian masses. Abdominal washing cytology revealed the presence of histiocytes with evidence of emperipolesis (Fig. 3). Bilateral salpingo-oophorectomy was performed as it was difficult to recognize the boundary between the lesion and the normal ovarian tissue, and to perform extirpation. The final pathological review of the specimen confirmed the results of the intraoperative frozen-section examination of the affected tissues of both ovaries: mononuclear and multinuclear polygonal histiocytes with evidence of emperipolesis were seen (Fig. 4), and the specimen was positive for S-100 protein and CD68. The patient was discharged 10 days after the surgery when her CRP level was normal; she was prescribed estrogen-replacement therapy. She has been doing well and has not shown any evidence of local recurrence for 24 months after surgery.

Discussion

While more than 600 cases of RDD have been reported, we believe this is the first reported case of extranodal RDD involving the ovaries. It is possible that the ovarian involvement was caused by implantation of the cells from the lesion in the CNS via the VP shunt because histiocytes were present in the abdominal washing cytological specimens, and this may have led to intra-abdominal relapse of RDD. When a VP shunt is placed for the management of hydrocephalus and viable cells of any type from the lesion in the CNS are present in the cerebrospinal fluid, a potential pathway is created for implantation of these cells through the shunt to the abdomen.

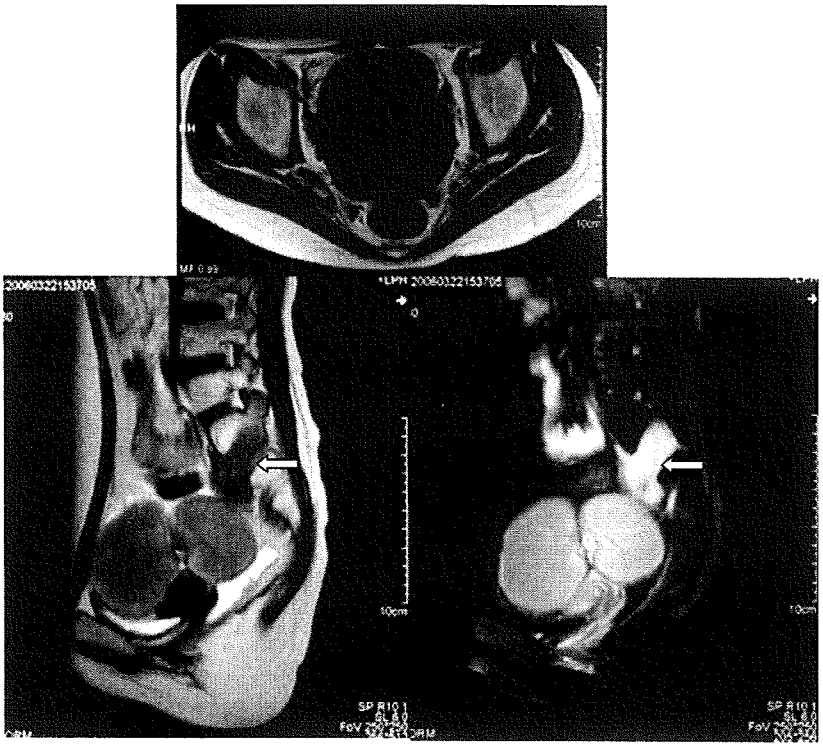

Figure 2 A magnetic resonance image showing pelvic masses. Top: T1-weighted axial image; left: T2-weighted sagittal image; and right: contrast-enhanced sagittal image. The sacral lesion, which was irradiated when the patient was 16, was one of the multiple recurrent lesions in the spinal cord (indicated by an arrow).

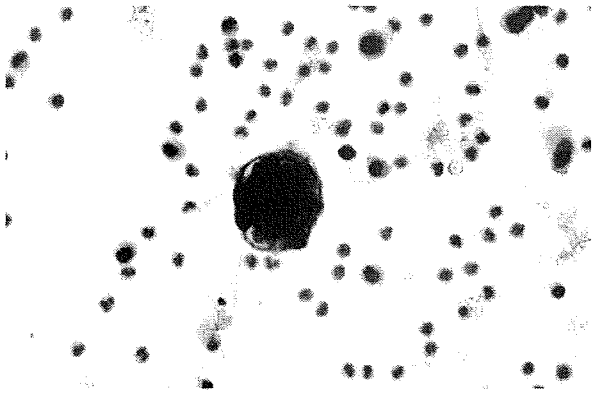

Figure 3 Photomicrograph of abdominal washing cytological specimen. Histiocytes exhibiting emperipolesis are seen (Giemsa stain, original magnification ×400).

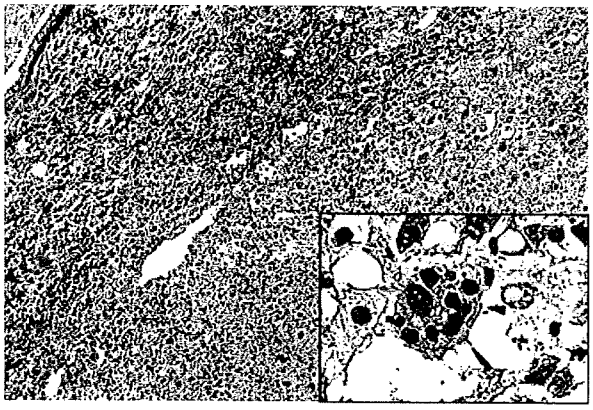

Figure 4 Histopathology slide of the ovarian tumor showing solid growths consisting of mononuclear and multinuclear polygonal histiocytes (hematoxylin and eosin stain, original magnification ×100). Emperipolesis is indicated by an arrowhead (inset, original magnification ×400).

Indeed, VP shunt-related abdominal metastases have been reported for many types of brain neoplasms, including medulloblastoma and other primitive neuroectodermal tumors, astrocytoma, germinoma, oligodendroglioma, ganglioglioma, ependymoma and melanoma.[6] However, VP shunt-related recurrence of RDD has not been reported before. Thus, it is possible that RDD recurred because of implantation of lesion cells into the abdominal cavity through the VP shunt – a phenomenon that has been observed in the case of other cerebral neoplasms.

Radiotherapy for RDD has been reported to show limited efficacy, while chemotherapy is in general ineffective.[7] Surgical resection is considered necessary in patients with impaired function of vital organs and/or with extranodal localization manifesting as important clinical signs. RDD generally has a favorable prognosis, but some patients have a chronic course with stable or progressive disease. In contrast to RDD involving a single lymph node region, RDD involving extranodal or multiple sites usually has a protracted course. It has been reported that when the surgical margins are involved, local recurrence is likely. This suggests that surgery with disease-free margins is crucial for locoregional control.[8,9] In our case, the preservation of normal ovarian tissue was difficult, and oophorectomy was performed to avoid local recurrence. However, extirpation of the lesion should be considered when appropriate and technically feasible.

This case illustrates the importance of considering metastatic disease in a patient in whom a VP shunt has been implanted. Doctors should keep in mind that RDD might recur because of implantation of lesion cells into the abdominal cavity through a VP shunt, as is known to occur in the case of cerebral neoplasms.

References

1. Rosai J, Dorfman RF. Sinus histiocytosis with massive lymphadenopathy: A newly recognized benign clinicopathological entity. *Arch Pathol* 1969; **87**: 63–70.
2. Foucar E, Rosai J, Dorfman R. Sinus histiocytosis with massive lymphadenopathy (Rosai–Dorfman disease): Review of the entity. *Semin Diagn Pathol* 1990; **7**: 19–73.
3. Cossor F, Al-Khater AH, Doll DC. Laryngeal obstruction and hoarseness associated with Rosai–Dorfman disease. *J Clin Oncol* 2006; **24**: 1953–1955.
4. Murray J, Fox H. Rosai–Dorfman disease of the uterine cervix. *Int J Gynecol Pathol* 1991; **10**: 209–213.
5. Knox SK, Kurtin PJ, Steensma DP. Isolated splenic sinus histiocytosis (Rosai–Dorfman disease) in association with myelodysplastic syndrome. *J Clin Oncol* 2006; **24**: 4027–4028.
6. Donovan DJ, Prauner RD. Shunt-related abdominal metastases in a child with choroid plexus carcinoma: Case report. *Neurosurgery* 2005; **56**: E412; discussion E412.
7. Pulsoni A, Anghel G, Falcucci P *et al.* Treatment of sinus histiocytosis with massive lymphadenopathy (Rosai–Dorfman disease): Report of a case and literature review. *Am J Hematol* 2002; **69**: 67–71.
8. Brenn T, Calonje E, Granter SR *et al.* Cutaneous Rosai–Dorfman disease is a distinct clinical entity. *Am J Dermatopathol* 2002; **24**: 385–391.
9. Cheng SP, Jeng KS, Liu CL. Subcutaneous Rosai–Dorfman disease: Is surgical excision justified? *J Eur Acad Dermatol Venereol* 2005; **19**: 747–750.

Gene expression profiling of advanced-stage serous ovarian cancers distinguishes novel subclasses and implicates *ZEB2* in tumor progression and prognosis

Kosuke Yoshihara,[1,10] Atsushi Tajima,[2,10] Dai Komata,[1] Tadashi Yamamoto,[3] Shoji Kodama,[4] Hiroyuki Fujiwara,[5] Mitsuaki Suzuki,[5] Yoshitaka Onishi,[6] Masayuki Hatae,[6] Kazunobu Sueyoshi,[7] Hisaya Fujiwara,[8] Yoshiki Kudo,[8] Ituro Inoue[2,9] and Kenichi Tanaka[1,9]

[1]Department of Obstetrics and Gynecology, Niigata University Graduate School of Medical and Dental Sciences, Niigata; [2]Department of Molecular Life Science, Tokai University School of Medicine, Isehara, Japan; [3]Department of Structural Pathology, Institute of Nephrology, Niigata University Graduate School of Medical and Dental Sciences; [4]Department of Gynecology, Niigata Cancer Center Hospital, Niigata; [5]Department of Obstetrics and Gynecology, Jichi Medical University, Shimotuke; [6]Department of Obstetrics and Gynecology, Kagoshima City Hospital; [7]Department of Pathology, Kagoshima City Hospital, Kagoshima; [8]Department of Obstetrics and Gynecology, Hiroshima University Graduate School of Biomedical Sciences, Hiroshima, Japan

(Received January 30, 2009/Revised April 16, 2009/Accepted April 24, 2009/Online publication May 26, 2009)

To elucidate the mechanisms of rapid progression of serous ovarian cancer, gene expression profiles from 43 ovarian cancer tissues comprising eight early stage and 35 advanced stage tissues were carried out using oligonucleotide microarrays of 18 716 genes. By non-negative matrix factorization analysis using 178 genes, which were extracted as stage-specific genes, 35 advanced stage cases were classified into two subclasses with superior (n = 17) and poor (n = 18) outcome evaluated by progression-free survival (log rank test, P = 0.03). Of the 178 stage-specific genes, 112 genes were identified as showing different expression between the two subclasses. Of the 48 genes selected for biological function by gene ontology analysis or Ingenuity Pathway Analysis, five genes (*ZEB2*, *CDH1*, *LTBP2*, *COL16A1*, and *ACTA2*) were extracted as candidates for prognostic factors associated with progression-free survival. The relationship between high *ZEB2* or low *CDH1* expression and shorter progression-free survival was validated by real-time RT-PCR experiments of 37 independent advanced stage cancer samples. *ZEB2* expression was negatively correlated with *CDH1* expression in advanced stage samples, whereas *ZEB2* knockdown in ovarian adenocarcinoma SKOV3 cells resulted in an increase in *CDH1* expression. Multivariate analysis showed that high *ZEB2* expression was independently associated with poor prognosis. Furthermore, the prognostic effect of E-cadherin encoded by *CDH1* was verified using immunohistochemical analysis of an independent advanced stage cancer samples set (n = 74). These findings suggest that the expression of epithelial–mesenchymal transition-related genes such as *ZEB2* and *CDH1* may play important roles in the invasion process of advanced stage serous ovarian cancer. (*Cancer Sci* 2009; 100: 1421–1428)

The serous type, comprising approximately 50% of ovarian cancers, is the most aggressive histology and has a tendency to be detected as advanced stage at the time of diagnosis.[1,2] Patients with advanced stage serous ovarian cancer are managed with surgical cytoreduction followed by platinum and taxane-based chemotherapy. Serous ovarian cancer is moderately chemosensitive and initially responds to postoperative chemotherapy, but the survival of patients with advanced stage remains poor. Because the majority of early stage ovarian cancers are asymptomatic and there is as yet no reliable screening test, it is difficult to diagnose early stage serous ovarian cancer. Therefore, the molecular mechanisms of progression in serous ovarian cancer should provide valuable clues for early detection and improved prognosis.

The development of microarray technology permits analysis of the expression levels of thousands of genes in cancer cells, and several studies have shown that microarrays can be used to identify gene expression profiles associated with surgery outcome, response to chemotherapy, grade, and survival in ovarian cancers.[3–17] However, there are limited reports of microarray analysis on tumor progression.[18–20] Serous ovarian cancer more rapidly progresses to advanced stage than other histological types.[21] In the present study, we used genome-wide expression microarray to distinguish between stage I (ovary confined) and stage III/IV serous ovarian cancers to focus on the molecular mechanisms of tumor progression and metastasis. Our microarray analysis identified 178 stage-specific genes, and also divided advanced stage (stage III/IV) ovarian cancers into two novel prognostic subclasses, by the NMF method. There were significant differences between the two subclasses in progression-free survival time. Furthermore, we extracted *CDH1* and its transcriptional repressor *ZEB2* from the 112 genes that were differentially expressed between the two novel subclasses, and found that the expression levels of these epithelial–mesenchymal transition-related genes[22,23] are associated with tumor progression and prognosis in advanced stage serous ovarian cancer patients.

Materials and Methods

Tissue samples. Eighty-nine patients (17 stage I; 72 stage III/IV) who were diagnosed with serous histological type ovarian cancer between July 1997 and October 2007 were recruited in this study. Fresh-frozen samples were obtained from primary tumor tissues at initial cytoreductive surgery. No patients received chemotherapy before surgery. All patients with advanced stage serous ovarian cancer (n = 72) were treated with platinum and taxane-based chemotherapy after surgery. The ethics committees of the participating institutions approved the study protocol, and each participant gave written, informed consent. Of the 89 samples, 43 were analyzed with microarray. The remaining 46 samples were used for subsequent validation analysis. There were no significant differences between the two samples sets regarding age of onset, stage, performance of optimal cytoreduction, histological grade, and follow-up period between the microarray set and validation set (Supplementary Table 1). Staging of the disease was assessed in accordance with the criteria of the International Federation of Gynecology and Obstetrics.[24] Optimal cytoreduction was defined as ≤1 cm of gross residual disease. The histological characteristics of surgically resected specimens

[9]To whom correspondence should be addressed.
E-mail: tanaken@med.niigata-u.ac.jp or ituro@is.icc.u-tokai.ac.jp
[10]These authors contributed equally to this work.

doi: 10.1111/j.1349-7006.2009.01204.x

were assessed on formalin-fixed and paraffin-embedded hematoxylin–eosin sections, and frozen tissues containing more than 80% tumor cells were used for RNA extraction. Normal peritoneum tissues were obtained from 10 patients having other procedures (such as hysterectomy for myoma uteri) at Niigata University. Tumors of 43 samples used for microarray analysis were screened for the presence of *TP53* somatic mutations using previously reported methods.[25] Four patients with family history of ovarian cancer in the microarray set were examined for germline mutations of *BRCA1* according to an in-house protocol,[26] and two patients showed mutations of *BRCA1*.

Microarray experiments. Total RNA, extracted from tissue samples using TRIzol reagent (Invitrogen, Carlsbad, CA, USA) was examined with a 2100 Bioanalyzer (Agilent Technologies, Palo Alto, CA, USA) using an RNA 6000 Nano LabChip (Agilent Technologies). Five hundred nanograms of total RNA was converted into labeled cRNA with nucleotides coupled to Cy3 (PerkinElmer, Boston, MA, USA) using the Low RNA Input Fluorescent Linear Amplification Kit (Agilent Technologies). Cy3-labeled cRNA (1.5 μg) was hybridized for 17 h at 65°C to an Agilent Human 1A (v2) Oligo Microarray, which carries 60-mer probes to 18 716 human transcripts. The hybridized microarray was washed and then scanned in Cy3 channel with the Agilent DNA Microarray Scanner (model G2565AA). Signal intensity per spot was generated from the scanned image with Feature Extraction Software version 8.5 (Agilent Technologies) with the default settings. Spots that did not pass quality control procedures were flagged as 'absent'.

Microarray data analysis. Data normalization was carried out using GeneSpring GX 7.3 (Agilent Technologies) as follows: (i) values below 0.01 were set to 0.01, following background subtraction; and (ii) median percentile normalization was carried out using a per-chip 50th percentile of all measurements. Furthermore, genes with expression levels marked as 'absent' in more than 22 of 43 microarrays were excluded to analyze ovarian cancer-specific transcripts. When the gene expression patterns of two groups were compared, genes showing twofold or more mean expression differences between the groups were first determined by Welch's *t*-test in GeneSpring GX. For multiple testing corrections in this statistical analysis, the Benjamini–Hochberg procedure[27] of controlling the false discovery rate at the level of 0.05 was used.

To assess heterogeneity of the gene expression profile among serous ovarian cancer patients, we applied a NMF algorithm and hierarchical clustering using stage-specific gene expression profiles. NMF analysis was carried out according to Brunet *et al.*[28] as previously reported.[29]

To investigate the biological functions of the gene expression profiles, we used GO Ontology Browser, embedded in GeneSpring GX, and IPA (http://www.ingenuity.com). More detailed information about this analysis using the GO Ontology Browser and IPA is given in Supplementary methods.

Quantitative RT-PCR analysis. Total RNA (1 μg) from ovarian cancer was used as a template in first-strand cDNA synthesis with the SuperScript III First-Strand Synthesis System (Invitrogen). The cDNA was diluted one in ten for subsequent real-time PCR, which was carried out using TaqMan Gene Expression Assays (Applied Biosystems) with TaqMan Universal PCR Master Mix (Applied Biosystems) on a 7900HT Sequence Detection System (Applied Biosystems) according to the manufacturers' instructions. Detailed information on the 23 transcripts examined is summarized in Supplementary Table 2. The relative quantification method[30] was used to measure the amounts of the respective genes in serous ovarian cancer samples, normalized to *ACTB* and *TBP*.

Analysis of clinical and pathological parameters. All analyses except Cox's proportional hazard analysis were done using GraphPad PRISM version 4.0 (GraphPad Software, San Diego, CA, USA). Survival curves were investigated using the Kaplan–Meier method and log rank test (GraphPad PRISM). When clinicopathological parameters among ovarian cancer patients were compared, unpaired *t*-test, Fisher's exact test or χ^2-test was used depending on the purpose (GraphPad PRISM). Pearson's correlation coefficient was calculated for correlation between *ZEB2* expression and *CDH1* expression. Differences in gene expression levels between two subclasses were tested by Mann–Whitney test. Using a $\log_2$ transformation of expression data, Cox's proportional hazard model analysis was carried out using JMP version 6 (SAS Institute, Cary, NC, USA).

Results

Identification and characterization of molecular subclasses from advanced stage serous ovarian cancer cases. Using Agilent Human 1A(v2) Oligo microarray, we generated gene expression data for 43 serous ovarian cancers comprising eight stage I and 35 stage III/IV tumors, as well as 10 normal peritoneum tissues as a reference. First, 4275 ovarian cancer-specific genes that were differentially expressed between ovarian cancer and peritoneum tissues were isolated. Of these 4275 transcripts, 178 stage-specific genes showing significantly more than twofold upregulation or downregulation in stage III/IV samples compared to stage I samples; 107 transcripts were upregulated and 71 transcripts downregulated in stage III/IV serous ovarian cancers (Supplementary Fig. 1).

To clarify the heterogeneity of the samples at the transcriptome level, 43 serous ovarian cancer samples were analyzed by the NMF method[28,29,31] using the 178 transcriptomes that were differentially expressed between stage I samples and stage III/IV samples. Figure 1(A) shows reordered consensus matrices averaging 50 connective matrices generated for subclasses $K = 2$, 3, 4, and 5. The most distinct pattern of block partitioning was observed at the $K = 2$ model. Thus, the NMF method predicts the existence of robust subclasses of serous ovarian cancer samples for $K = 2$. This prediction was quantitatively supported by higher values of coph for NMF-clustered matrices. The NMF class assignment for $K = 2$ was the most robust with the highest coph value (coph = 0.999). Interestingly, one subclass in the $K = 2$ model was composed of eight stage I samples and 17 stage III/IV samples, whereas the other was composed of 18 stage III/IV samples. To verify the accuracy and robustness of the classification, a hierarchical clustering approach was also applied to log-transformed normalized data for stage-specific target genes. As depicted in Figure 1(B), 43 serous ovarian cancer samples were separated into two main branches showing similarity with the NMF-based subclassification. Thus, it was confirmed that the 35 advanced stage serous ovarian cancer samples were categorized into two distinct subclasses at the transcriptome level. A group composed of 17 stage III/IV samples with gene expression profiles similar to stage I samples was termed 'subclass 1', and the second group comprising 18 stage III/IV samples was termed 'subclass 2'. Two patients were identified as harboring *BRCA1* mutations: one patient belonged to stage I and the other to subclass 1 in the array analysis, but there was no particular gene expression pattern due to the mutations based on the expression levels of the 178 stage-specific genes.

We then investigated the possibility that the two subclasses of advanced stage serous ovarian cancers split by the NMF approach might represent clinically, pathologically, or genetically distinct characteristics. The distribution of several known prognostic factors is listed in Table 1. The two subclasses were similar in age of onset, stage, CA125 level before treatment, presence of tumor cells in ascites, histological grade, presence of lymph node metastasis, and frequency of *TP53* mutations, except that subclass 1 had a higher rate of optimal cytoreduction than subclass 2 (Fisher's exact test, $P = 0.09$). When the outcome of two

doi: 10.1111/j.1349-7006.2009.01204.x

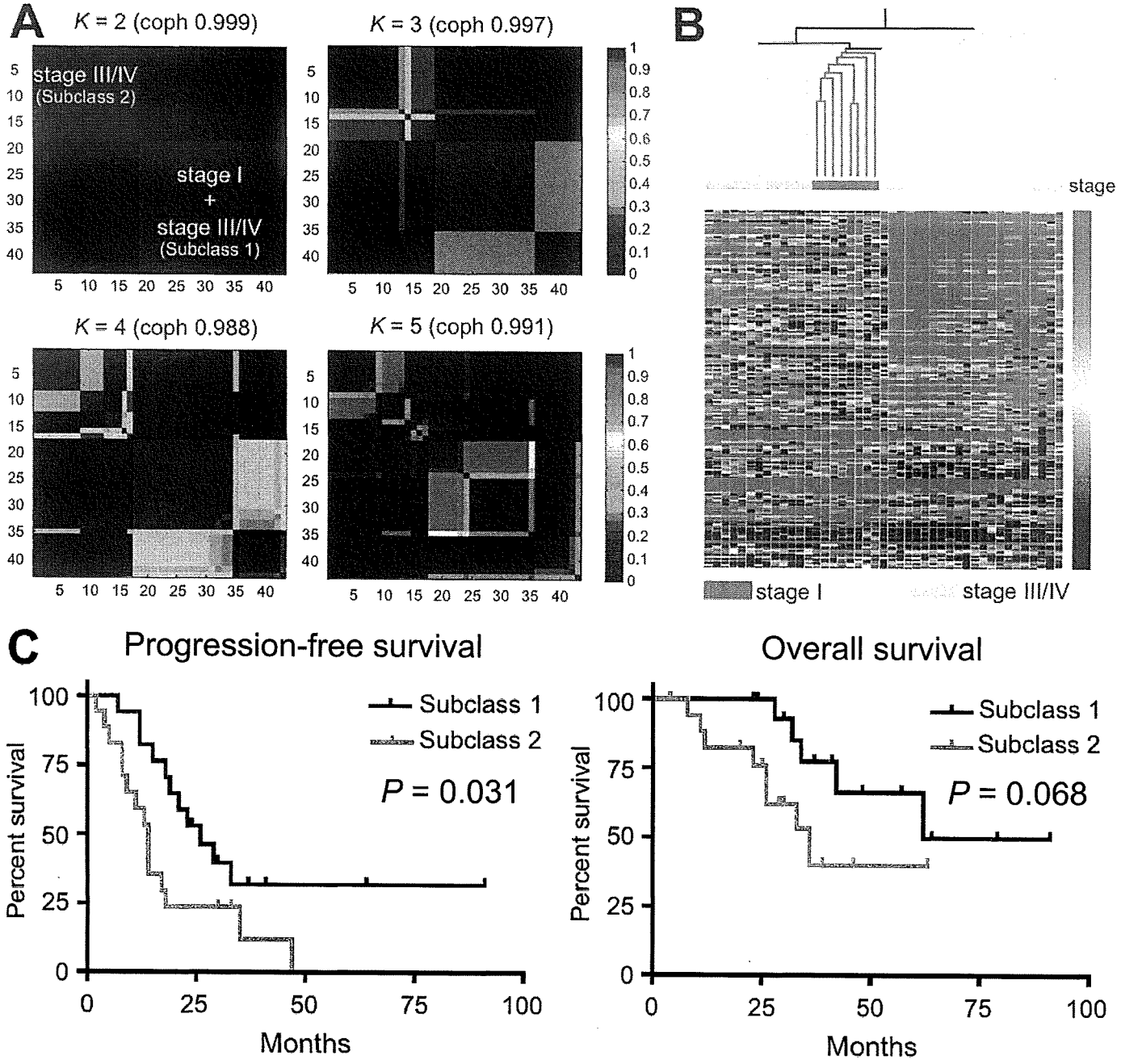

Fig. 1. Subclassification of 43 serous ovarian cancer samples and their prognosis. (A) By a non-negative matrix factorization (NMF) approach, NMF-consensus matrices averaging 50 connectivity matrices were computed at $K = 2$–5 (as the number of subclasses modeled) for the 43 serous ovarian cancer samples with 178 stage-specific genes. The NMF computation and model selection were carried out according to Brunet *et al.*[28] By accounting for the cophenetic correlation coefficients (coph) for NMF-clustered matrices, the NMF class assignment at $K = 2$ was the most robust. One subclass in the $K = 2$ model contained samples both from stage I ($n = 8$) and III/IV ($n = 17$), whereas the other contained only stage III/IV samples ($n = 18$). (B) A hierarchical clustering method was also used to classify serous ovarian cancer samples using 178 stage-specific genes. The 43 serous samples were largely separated into two clusters. The stage assignments for samples are: stage I, red; and stage III/IV, yellow. (C) Kaplan–Meier survival curves between two NMF-based subclasses of the 35 stage III/IV patients. Subclass 1, composed of 17 advanced stage patients with gene expression profiles similar to that of stage I, showed statistically prolonged progression-free survival (log rank test, $P = 0.031$), but no significant correlation with overall survival (log rank test, $P = 0.068$).

subclasses was compared for progression-free survival and overall survival, the Kaplan–Meier curves showed significantly better outcome in cases belonging to subclass 1 in progression-free survival (Fig. 1C, log rank test, $P = 0.031$) and fair outcome in overall survival (Fig. 1C, log rank test, $P = 0.068$).

Association of subclass-specific gene expression profile with prognosis of ovarian cancer patients. To characterize the gene expression differences associated with distinct prognoses between the two subclasses of advanced stage serous ovarian cancers, we identified 112 subclass-specific transcripts that were differentially expressed between the two subclasses; 25 transcripts were up-regulated in subclass 1 and 87 transcripts were upregulated in subclass 2 (Supplementary Table 3). We then examined the biological functions of the 112 subclass-specific genes using two analytic tools, GO analysis and IPA, to clarify the biological mechanism of tumor progression. The Gene Ontology Biological

Table 1. Clinical characteristics of two subclasses of advanced stage serous ovarian cancer samples

Characteristic	Subclass 1 ($n = 17$)	Subclass 2 ($n = 18$)	*P*-value
Age (years)	58.5 ± 8.6	61.1 ± 12.6	0.49†
Stage			
Stage III	16	15	1‡
Stage IV	1	3	
CA125 (IU)	1987 ± 2021	1178 ± 1057	0.14†
Cancer cell in abdominal fluid			
Positive	15	15	1‡
Negative	2	3	
Optimal cytoreduction			
Optimal (<1 cm)	12	7	0.09‡
Not optimal	5	11	
Lymph node metastasis			
Positive	6	4	1‡
Negative	9	6	
Unknown	2	8	
Grade			
Grade 1	6	4	0.18§
Grade 2	9	7	
Grade 3	2	7	
TP53 status			
Wild type	11	9	0.50‡
Mutated	6	9	

Differences in clinical characteristics between subclass 1 and subclass 2 were tested using the †unpaired *t*-test, ‡Fisher's exact test or §χ^2-test.

Table 2. Univariable Cox's proportional hazards model analysis of expression levels of five genes for progression-free survival and overall survival in patients with advanced stage serous ovarian cancers

Gene symbol	Hazard ratio (95% CI)	*P*-value
Microarray set (n = 35)		
Progression-free survival		
ZEB2	1.35 (1.06–1.77)	0.015*
CDH1	0.75 (0.62–0.94)	0.017*
LTBP2	1.63 (1.04–2.57)	0.032*
COL16A1	1.33 (1.02–1.74)	0.034*
ACTA2	1.21 (1.01–1.46)	0.036*
Overall survival		
ZEB2	1.56 (1.06–2.47)	0.023*
CDH1	0.81 (0.67–1.03)	0.081
LTBP2	2.53 (1.43–4.58)	0.0017*
COL16A1	1.66 (1.12–2.59)	0.012*
ACTA2	1.44 (1.10–1.95)	0.0087*
Validation set (n = 37)		
Progression-free survival		
ZEB2	1.74 (1.08–2.92)	0.023*
CDH1	0.20 (0.09–0.45)	0.00006*
LTBP2	1.16 (0.75–1.75)	0.49
COL16A1	1.18 (0.92–1.51)	0.20
ACTA2	1.22 (0.90–1.66)	0.19
Overall survival		
ZEB2	1.89 (1.06–3.64)	0.029*
CDH1	0.59 (0.26–1.30)	0.19
LTBP2	1.1 (0.70–1.66)	0.69
COL16A1	1.23 (0.93–1.66)	0.15
ACTA2	1.43 (0.99–2.13)	0.052

*$P < 0.05$.

Process categories over-represented among 112 subclass-specific genes are shown in Figure 2(A). After multiple testing corrections using the Benjamini–Hochberg FDR method, seven categories were significantly over-represented, and included 37 non-overlapping genes. Subclass-specific genes were involved in biological processes of transport (GO6817, GO15698, GO6820, and GO6811), development (GO48513 and GO1501), and cell adhesion (GO7155), and included a high proportion of extracellular matrix-related genes. In addition, when ID of Agilent probes of 112 subclass-specific transcripts were imported into the IPA software, a new pathway comprising 26 genes that were enriched in extracellular matrix genes was identified (Fig. 2B). Fifteen genes belonged to both the seven GO categories and the new network, and 48 non-redundant genes were biologically characterized.

To investigate whether the expression profile of the 48 genes extracted by GO analysis or IPA was implicated in the aggressive phenotype of ovarian cancer, we analyzed the association between the respective expression levels of the 48 genes and progression-free survival time using univariate Cox's proportional hazard model. The expression levels of *ZEB2*, *CDH1*, *LTBP2*, *COL16A1*, and *ACTA2* were significantly correlated with progression-free survival (Table 2). When overall survival also was evaluated by Cox's proportional hazard model, the expression of the above genes except *CDH1* was significantly correlated with overall survival.

Validation by quantitative real-time RT-PCR. To validate the microarray expression data, we measured expression levels of 23 randomly selected transcripts from the 112 subclass-specific transcripts by real-time RT-PCR analysis. In agreement with microarray results, there was a significant difference between the expression levels of the 23 transcripts measured by real-time RT-PCR of subclass 1 and subclass 2 (Supplementary Table 4).

To validate the previous findings that the expression levels of *ZEB2*, *CDH1*, *LTBP2*, *COL16A1*, and *ACTA2* are associated with progression-free survival, quantitative real-time RT-PCR was carried out on 46 samples comprising nine stage I samples and 37 stage III/IV samples recruited as an independent validation set. Cox's proportional hazard analysis showed that the expression levels of *ZEB2* and *CDH1* were again correlated with progression-free survival ($P = 0.023$ and 0.00006, respectively) (Table 2). Moreover, *ZEB2* expression was significantly associated with overall survival ($P = 0.029$). At the protein level, an association of the expression of E-cadherin (encoded by *CDH1*) with prognosis of advanced stage serous ovarian cancer patients was further verified by immunohistochemical analysis of independent samples ($n = 74$) (Supplementary Fig. 3) as previously reported.[32–35]

Interaction between *ZEB2* and *CDH1*. *ZEB2* directly interacted with *CDH1* in the IPA network, as shown in Figure 2(B). We also found a significantly negative correlation between *ZEB2* expression and *CDH1* expression (Pearson's correlation coefficient: –0.432, $P = 0.0002$) in advanced stage serous ovarian cancers using real-time RT-PCR data ($n = 72$). *ZEB2* acts on the promoter of *CDH1*, a well-known epithelial marker, and reduces its expression.[23,36] To confirm the interaction between *ZEB2* and *CDH1* in ovarian cancer cells, a siRNA approach was used. For this purpose, we selected the SKOV3 cell line expressing endogenously higher *ZEB2* and lower *CDH1* mRNA than other ovarian cancer cell lines (Supplementary Fig. 3A,B). In SKOV3 cells, siRNA-mediated transient silencing of *ZEB2* expression resulted in upregulation of *CDH1* expression and downregulation of *FN1* and *VIM* expression (Supplementary Fig. 3C–F).

For multivariate analysis, we selected *ZEB2* from the two genes as likely to be the more important prognostic factor owing to its functional significance as an upstream repressor of *CDH1*.[23] The prognostic capability of *ZEB2* was further compared with other prognosis-related variables such as clinicopathological factors including age, performance of optimal cytoreduction, and histological grade using multivariate Cox's proportional

doi: 10.1111/j.1349-7006.2009.01204.x

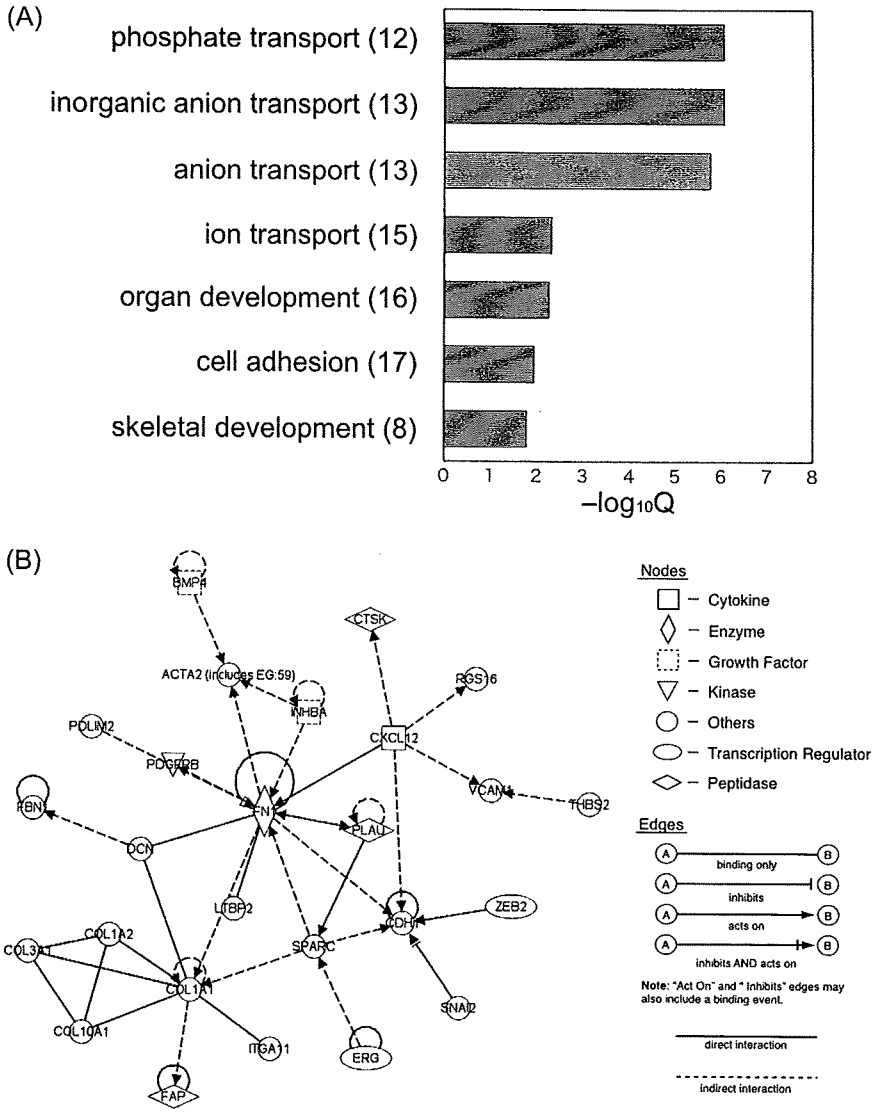

Fig. 2. Biological characterization of 112 subclass-specific genes using Gene Ontology analysis and Ingenuity Pathway Analysis (IPA). (A) Significant enrichments of gene ontology (GO) categories in GO-based profiling of 112 subclass-specific genes. Gray bars represent *q*-values (expressed as the negative logarithm [base 10]) after multiple testing correction of the Benjamini–Hochberg false discovery rate method for the significant ($q < 0.05$) GO categories over-represented in the 112 subclass-specific genes, using 4275 ovarian cancer-specific genes as a background set of genes for the determination of *q*-values. The actual number of the subclass-specific genes involved in each category is given in parentheses. (B) Twenty-six of 112 (24.1%) genes appeared in a new network based on the Ingenuity Pathway Knowledge base. Nodes represent genes, with their shapes showing IPA-defined functional classes of genes, and edges indicating biological relationships between nodes.

hazards analysis (Table 3). To increase the reliability of the multivariate analyses, all of the advanced stage serous ovarian cancer samples ($n = 72$) were analyzed by the real-time PCR technique. In Cox's proportional hazards model, *ZEB2* expression and the rate of optimal cytoreduction surgery were independent factors for progression-free survival time ($P = 0.014$ and 0.0011 respectively). The hazard ratio for relapse of *ZEB2* expression was 1.37 (95% confidence interval 1.07–1.78). Furthermore, when overall survival was evaluated by multivariate analysis, only the *ZEB2* expression level was independently associated with overall survival time ($P = 0.027$, hazard ratio = 1.53, 95% confidence interval 1.05–2.22).

***ZEB2* and *CDH1* expression and survival.** To clarify the details of the *ZEB2–CDH1* relationship, we analyzed the prognostic implications with regard to combinations of *ZEB2* and *CDH1* expression. For this purpose, we divided all of the samples into four groups, as shown in Table 4, when using a median expression level of each gene as a threshold for sample division. Multivariate Cox's proportional hazard model was used to compare survival among these four groups. The group showing high expression of *CDH1* and low expression of *ZEB2* served as a reference. Of the four groups, the only group with low expression of *CDH1* and high expression of *ZEB2* showed significantly poor prognosis in both progression-free survival and overall survival ($P = 0.0035$ and 0.013 respectively). When *ZEB2* expression was analyzed in combination with *CDH1* expression, the prognostic power of these genes became more significant.

Discussion

In this study, we evaluated the global gene expression profile to clarify the molecular etiology of the rapid progression specific to serous histological type cancers. We first attempted to subclassify our 43 serous type ovarian cancer tissues comprising eight stage I samples and 35 stage III/IV samples by a stepwise extraction of genes reflecting expression differences between samples (Supplementary Fig. 1). Although various classification methods have been proposed to characterize various cancer types at the molecular level using gene expression data, most of the methods tend to be unstable, producing different clusters with slightly different input or different choice of initial conditions.[37] Brunet *et al.*[28] showed that NMF is able to recover biologically significant phenotypes and appears superior to other methods especially when prior knowledge is lacking or undetermined. By applying the NMF algorithm, 35 patients with advanced stage serous ovarian cancer were grouped into two subclasses with 112 subclass-specific genes representing unique characteristics of tumor progression. Interestingly, one subclass, subclass 1 ($n = 17$), with a gene expression profile similar to that of stage I, showed a favorable outcome compared to the other subclass,

Table 3. Multivariable Cox's proportional hazards model analysis of prognostic factors for progression-free survival and overall survival in patients with advanced stage serous ovarian cancers ($n = 72$)

Variable	Hazard ratio (95% CI)	*P*-value
Progression-free survival		
ZEB2 expression	1.37 (1.07–1.78)	0.014*
Age	0.98 (0.96–1.00)	0.095
Optimal surgery (vs not optimal)	0.60 (0.44–0.82)	0.0011*
Grade 2 (vs Grade 1)	0.85 (0.58–1.24)	0.42
Grade 3 (vs Grade 1)	1.41 (0.98–2.06)	0.060
Overall survival		
ZEB2 expression	1.53 (1.05–2.22)	0.027*
Age	1.01 (0.96–1.04)	0.71
Optimal surgery (vs not optimal)	0.67 (0.41–1.05)	0.079
Grade 2 (vs Grade 1)	0.83 (0.47–1.50)	0.53
Grade 3 (vs Grade 1)	1.51 (0.93–2.62)	0.10

*Statistically significant ($P < 0.05$).

Table 4. Comparison of progression-free survival and overall survival in four groups with different expression profiles of *CDH1* and *ZEB2*

Serous ovarian cancer ($n = 72$)	Hazard ratio	95% CI	*P*-value
Progression-free survival			
CDH1 high/*ZEB2* low ($n = 23$)	1.00		
CDH1 high/*ZEB2* high ($n = 13$)	0.91	(0.53–1.43)	0.69
CDH1 low/*ZEB2* low ($n = 13$)	1.29	(0.83–1.94)	0.25
CDH1 low/*ZEB2* high ($n = 23$)	1.65	(1.18–2.35)	0.0035*
Overall survival			
CDH1 high/*ZEB2* low ($n = 23$)	1.00		
CDH1 high/*ZEB2* high ($n = 13$)	0.96	(0.37–1.96)	0.91
CDH1 low/*ZEB2* low ($n = 13$)	1.12	(0.63–1.95)	0.70
CDH1 low/*ZEB2* high ($n = 23$)	1.77	(1.12–2.92)	0.013*

subclass 2 ($n = 18$). This result was compatible with findings by Berchuck *et al.*[7] demonstrating similarities in gene expression between early stage serous ovarian cancers and a subset of advanced stage serous ovarian cancers that had favorable prognosis. Regarding the sample size in the current microarray analysis, one can realize that this may be first-stage evidence on ovarian expression profile associated with tumor progression. However, we successfully provided valuable insights that clarify the molecular mechanism of tumor progression using NMF algorithm.

Kurman *et al.* divide epithelial ovarian cancers into two groups designated type I and type II based on clinical, pathological, and molecular genetic studies.[21] Type I tumors are low grade and slow growing (including endometrioid, mucinous, and low-grade serous). Type II tumors (including high grade serous and undifferentiated) are rapidly growing, more aggressive, and are frequently associated with *TP53* mutation. In our experiments, the frequency of *TP53* mutation was higher in cases belonging to subclass 2 (9/18, 50%) compared to those belonging to subclass 1 + stage I (8/25, 32%). Although the frequency difference was not statistically significant, our novel subclassification based on gene expression profile might have a potential relationship with that of the two-type classification model of ovarian cancer proposed by Kurman *et al.*[21] Further study will be necessary to elucidate other biological and pathological implications except tumor progression in our subclassification.

After screening genes associated with tumor progression and subsequent validation of the association, we identified the expression of *ZEB2* and *CDH1* as prognostic factors for serous ovarian cancers. Although other genome-wide expression analyses[7–10] have identified gene expression profiles with prognosis values in patients with ovarian cancer, *ZEB2* and *CDH1* are not listed in their profiles. Previous studies using the expression microarrays investigate directly the association between gene expression level and survival time in patients with ovarian cancer, whereas we first extracted gene expression profiles reflecting tumor progression by a stepwise approach (Supplementary Fig. 1), and selected survival-associated genes with biological function from these genes. Furthermore, differences in microarray platforms, normalization methods, degrees of contamination by non-cancer cells in a given tumor specimen, and the patient populations under study[38] were observed between previous reports and ours. These points might contribute to the development of inconsistencies in lists of survival-associated genes from the microarray studies.

Our data also suggest that reduced *CDH1* expression is a key to subclassify advanced stage serous ovarian cancers. Recently Tothill *et al.* reported that six molecular subtypes of ovarian cancers, including serous and endometrioid histological types, were identified by a *k*-means clustering method according to genome-wide expression data from 285 ovarian cancer samples.[39] Of the six molecular subtypes, one subtype (C5 in the paper), comprising mainly high grade serous ovarian cancer samples, is characterized by reduced E-cadherin. Despite the difference in experimental design of the two studies, our data are compatible with their finding that a molecular subtype of ovarian cancers can be tagged by E-cadherin expression. E-cadherin is a hallmark of epithelial–mesenchymal transition, and a reduction of E-cadherin is thought to result in dysfunction of the cell–cell junction system, triggering cancer invasion in various human malignancies. In our experiment, E-cadherin expression was significantly associated with prognosis in patients with advanced stage serous ovarian cancer at both the mRNA and protein levels. Therefore, it is important to clarify the regulatory mechanisms of *CDH1* expression[40] in serous ovarian cancer in terms of tumor progression and prognosis, as well as subclassification.

Recent study shows that the interaction of Snail, ZEB, and bHLH factors regulates *CDH1* repression and epithelial–mesenchymal transition.[23] Besides *ZEB2*, other transcriptional repressors may reduce *CDH1* expression and lead to epithelial–mesenchymal transition.[41] Indeed, *SNAI2* was included in the 112 subclass-specific genes, and was found to directly interact with *CDH1* in the newly obtained IPA network (Fig. 2B). Previous reports show that other transcriptional repressors such as Snail 1 and Twist are related to prognosis in ovarian cancer, using immunohistochemical analysis.[35,42] Hosono *et al.*[42] have reported that expression of Twist is a significant prognostic factor in non-serous type but not in serous type tumors. Our results demonstrate that expression of *ZEB2* is negatively correlated with *CDH1* expression, and that the expression signature of increased *ZEB2* and reduced *CDH1* in ovarian tumor tissues is related to poor prognosis in serous ovarian cancer patients (Table 4). Furthermore, siRNA-mediated suppression of *ZEB2* in the serous type of ovarian cancer SKOV3 cells leads to an increase in *CDH1* expression (Supplementary Fig. 3), suggesting that *ZEB2* regulates *CDH1* expression in serous histological type tumors. To validate that *ZEB2* expression at the protein level is a significant prognostic factor, we would like to analyze *ZEB2* expression in a larger number of patients stratified according to individual histological types using immunohistochemical staining.

Park *et al.* have recently reported that microRNA-200 directly targets the mRNA of *ZEB2* as well as that of *ZEB1*, and indirectly controls the expression level of *CDH1* in cancer cell lines.[43] Further investigation is required to elucidate the more detailed mechanisms by which the *ZEB2–CDH1* axis in epithelial–mesenchymal transition is regulated in the process of ovarian cancer progression. Clarification of the mechanisms for the regulation of *ZEB2–CDH1* expression may provide plausible targets for the development of therapeutic strategies in the clinical management of serous ovarian cancers.

doi: 10.1111/j.1349-7006.2009.01204.x

Acknowledgments

This work was supported in part by a Grant-in-Aid for the Third-term Cancer Control Strategy Program from the Ministry of Health, Labor and Welfare, Japan. We are grateful to Hiroshi Kamiguchi and Tadayuki Satoh (Teaching and Research Support Center, Tokai University School of Medicine) for their technical support in the microarray experiment, and also thank Yoshiko Sakamoto, Eriko Tokubo, Hiromi Kamura, and Kozue Otaka for their technical assistance.

Abbreviations

ACTA2	actin, alpha 2, smooth muscle, aorta
ACTB	actin, beta
bHLH	basic helix-loop-helix
BRCA1	breast cancer 1, early onset
CA125	carbohydrate antigen 125
CDH1	cadherin 1
COL16A1	collagen, type XVI, alpha 1
coph	cophenetic correlation coefficient
Cy3	cyamine 3-CTP
FN1	fibronectin 1
GO	gene ontology
IPA	Ingenuity Pathway Analysis
LTBP2	latent transforming growth factor beta binding protein 2
NMF	non-negative matrix factorization
SNAI1	snail homolog 1
TBP	TATA box binding protein
TP53	Tumor Protein p53
VIM	vimentin
ZEB2	zinc finger E-box binding homeobox 2

References

1 Disaia PJ, Creasman WT. Epithelial ovarian cancer. In: Disaia PJ, Creasman WT, eds. *Clinical Gynecologic Oncology*, 6th edn. St Louis: Mosby, 2002; 289–350.
2 Cannistra SA. Cancer of the ovary. *N Engl J Med* 2004; **351**: 2519–29.
3 Agarwal R, Kaye SB. Expression profiling and individualization of treatment for ovarian cancer. *Curr Opin Pharmacol* 2006; **6**: 345–9.
4 Olivier RI, van Beurden M, van't Veer LJ. The role of gene expression profiling in the clinical management of ovarian cancer. *Eur J Cancer* 2006; **42**: 2930–8.
5 Fehrmann RS, Li XY, van der Zee AG *et al.* Profiling studies in ovarian cancer: a review. *Oncologist* 2007; **12**: 960–6.
6 Spentzos D, Levine DA, Ramoni MF *et al.* Gene expression signature with independent prognostic significance in epithelial ovarian cancer. *J Clin Oncol* 2004; **22**: 4700–10.
7 Berchuck A, Iversen ES, Lancaster JM *et al.* Patterns of gene expression that characterize long-term survival in advanced stage serous ovarian cancers. *Clin Cancer Res* 2005; **11**: 3686–96.
8 Hartmann LC, Lu KH, Linette GP *et al.* Gene expression profiles predict early relapse in ovarian cancer after platinum-paclitaxel chemotherapy. *Clin Cancer Res* 2005; **11**: 2149–55.
9 Bonome T, Levine DA, Shih J *et al.* A gene signature predicting for survival in suboptimally debulked patients with ovarian cancer. *Cancer Res* 2008; **68**: 5478–86.
10 Le Page C, Ouellet V, Quinn MC, Tonin PN, Provencher DM, Mes-Masson AM. BTF4/BTNA3.2 and GCS as candidate mRNA prognostic markers in epithelial ovarian cancer. *Cancer Epidemiol Biomarkers Prev* 2008; **17**: 913–20.
11 Dressman HK, Berchuck A, Chan G *et al.* An integrated genomic-based approach to individualized treatment of patients with advanced-stage ovarian cancer. *J Clin Oncol* 2007; **25**: 517–25.
12 Newton TR, Parsons PG, Lincoln DJ *et al.* Expression profiling correlates with treatment response in women with advanced serous epithelial ovarian cancer. *Int J Cancer* 2006; **119**: 875–83.
13 Partheen K, Levan K, Osterberg L, Horvath G. Expression analysis of stage III serous ovarian adenocarcinoma distinguishes a sub-group of survivors. *Eur J Cancer* 2006; **42**: 2846–54.
14 Okamoto A, Nikaido T, Ochiai K *et al.* Indoleamine 2,3-dioxygenase serves as a marker of poor prognosis in gene expression profiles of serous ovarian cancer cells. *Clin Cancer Res* 2005; **11**: 6030–9.
15 Donninger H, Bonome T, Radonovich M *et al.* Whole genome expression profiling of advance stage papillary serous ovarian cancer reveals activated pathways. *Oncogene* 2004; **23**: 8065–77.
16 Meinhold-Heerlein I, Bauerschlag D, Hilpert F *et al.* Molecular and prognostic distinction between serous ovarian carcinomas of varying grade and malignant potential. *Oncogene* 2005; **24**: 1053–65.
17 Bonome T, Lee JY, Park DC *et al.* Expression profiling of serous low malignant potential, low-grade, and high-grade tumors of the ovary. *Cancer Res* 2005; **65**: 10602–12.
18 Shridhar V, Lee J, Pandita A *et al.* Genetic analysis of early-versus late-stage ovarian tumors. *Cancer Res* 2001; **61**: 5895–904.
19 De Cecco L, Marchionni L, Gariboldi M *et al.* Gene expression profiling of advanced ovarian cancer: characterization of a molecular signature involving fibroblast growth factor 2. *Oncogene* 2004; **23**: 8171–83.
20 Lancaster JM, Dressman HK, Clarke JP *et al.* Identification of genes associated with ovarian cancer metastasis using microarray expression analysis. *Int J Gynecol Cancer* 2006; **16**: 1733–45.
21 Kurman RJ, Visvanathan K, Roden R, Wu TC, Shin IeM. Early detection and treatment of ovarian cancer: shifting from early stage to minimal volume disease based on a new model of carcinogenesis. *Am J Obstet Gynecol* 2008; **198**: 351–6.
22 Thiery JP. Epithelial mesenchymal transitions in tumour progression. *Nat Rev Cancer* 2002; **2**: 442–54.
23 Peinado H, Olmeda D, Cano A. Snail, Zeb and bHLH factors in tumour progression: an alliance against the epithelial phenotype? *Nat Rev Cancer* 2007; **7**: 415–28.
24 FIGO Cancer Committee. Staging Announcement: FIGO Cancer Committee. *Gynecol Oncol* 1986; **25**: 383–5.
25 Amikura T, Sekine M, Hirai Y *et al.* Mutational analysis of TP53 and p21 in familial and sporadic ovarian cancer in Japan. *Gynecol Oncol* 2006; **100**: 365–71.
26 Sekine M, Nagata H, Tsuji S *et al.* Mutational analysis of BRCA1 and BRCA2 and clinicopathologic analysis of ovarian cancer in 82 ovarian cancer families: two common founder mutations of BRCA1 in Japanese population. *Clin Cancer Res* 2001; **7**: 3144–50.
27 Benjamini Y, Hochberg Y. Controlling the false discovery rate: a practical and powerful approach to multiple testing. *J R Statist Soc B* 1995; **57**: 289–300.
28 Brunet JP, Tamayo P, Golub TR, Mesirov JP. Metagenes and molecular pattern discovery using matrix factorization. *Proc Natl Acad Sci USA* 2004; **101**: 4164–9.
29 Okada H, Tajima A, Shichiri K, Tanaka A, Tanaka K, Inoue I. Genome-wide expression of azoospermia testes demonstrates a specific profile and implicates ART3 in genetic susceptibility. *PLoS Genet* 2008; **4**: e26.
30 Livak KJ, Schmittgen TD. Analysis of relative gene expression data using real-time quantitative PCR and the 2–ΔΔCT method. *Methods* 2001; **25**: 402–8.
31 Inamura K, Fujiwara T, Hoshida Y *et al.* Two subclasses of lung squamous cell carcinoma with different gene expression profiles and prognosis identified by hierarchical clustering and non-negative matrix factorization. *Oncogene* 2005; **24**: 7105–13.
32 Daraï E, Scoazec JY, Walker-Combrouze F *et al.* Expression of cadherins in benign, borderline, and malignant ovarian epithelial tumors: a clinicopathologic study of 60 cases. *Hum Pathol* 1997; **28**: 922–8.
33 Faleiro-Rodrigues C, Macedo-Pinto I, Pereira D, Lopes CS. Prognostic value of E-cadherin immunoexpression in patients with primary ovarian carcinomas. *Ann Oncol* 2004; **15**: 1535–42.
34 Voutilainen KA, Anttila MA, Sillanpää SM *et al.* Prognostic significance of E-cadherin–catenin complex in epithelial ovarian cancer. *J Clin Pathol* 2006; **59**: 460–7.
35 Blechschmidt K, Sassen S, Schmalfeldt B, Schuster T, Höfler H, Becker KF. The E-cadherin repressor Snail is associated with lower overall survival of ovarian cancer patients. *Br J Cancer* 2007; **98**: 489–95.
36 Imamichi Y, König A, Gress T, Menke A. Collagen type I-induced Smad-interacting protein 1 expression downregulates E-cadherin in pancreatic cancer. *Oncogene* 2007; **26**: 2381–5.
37 Gao Y, Church G. Improving molecular cancer class discovery through sparse non-negative matrix factorization. *Bioinformatics* 2005; **21**: 3970–5.
38 Konstantinopoulos PA, Spentzos D, Cannistra SA. Gene-expression profiling in epithelial ovarian cancer. *Nat Clin Pract Oncol* 2008; **5**: 577–87.
39 Tothill RW, Tinker AV, George J *et al.* Novel molecular subtypes of serous and endometrioid ovarian cancer linked to clinical outcome. *Clin Cancer Res* 2008; **14**: 5198–208.
40 Liu YN, Lee WW, Wang CY, Chao TH, Chen Y, Chen JH. Regulatory mechanisms controlling human E-cadherin gene expression. *Oncogene* 2005; **24**: 8277–90.
41 Imai T, Horiuchi A, Wang C *et al.* Hypoxia attenuates the expression of E-cadherin via up-regulation of SNAIL in ovarian carcinoma cells. *Am J Pathol* 2003; **163**: 1437–47.

42 Hosono S, Kajiyama H, Terauchi M *et al.* Expression of Twist increases the risk for recurrence and for poor survival in epithelial ovarian carcinoma patients. *Br J Cancer* 2007; **96**: 314–20.

43 Park SM, Gaur AB, Lengyel E, Peter ME. The miR-200 family determines the epithelial phenotype of cancer cells by targeting the E-cadherin repressors ZEB1 and ZEB2. *Genes Dev* 2008; **22**: 894–907.

Supporting Information

Additional Supporting Information may be found in the online version of this article:

Fig. S1. Analytical process to extract 'subclass-specific genes'.

Fig. S2. Association between E-cadherin expression and prognosis of advanced stage serous ovarian cancers validated by immunohistochemical analyses.

Fig. S3. Interaction between *ZEB2* and *CDH1*.

Table S1. Comparison of clinicopathological characteristics between microarray set and validation set

Table S2. List of 23 transcripts analyzed by quantitative real-time RT-PCR in this study

Table S3. One hundred and twelve transcripts representing statistically significant expression differences between two subclasses of advanced stage serous ovarian cancers

Table S4. Expression levels of 23 genes by quantitative real-time RT-PCR were significantly different between subclass 1 (S1) and subclass 2 (S2)

Supplementary Methods Methods about GO analysis, Pathway analysis, siRNA experiments, and immunohistochemical analysis

Please note: Wiley-Blackwell are not responsible for the content or functionality of any supporting materials supplied by the authors. Any queries (other than missing material) should be directed to the corresponding author for the article.

doi: 10.1111/j.1349-7006.2009.01204.x

Menopause: The Journal of The North American Menopause Society
Vol. 16, No. 1, pp. 000-000
DOI: 10.1097/gme.0b013e31817ed24f

Relationship between single nucleotide polymorphisms in *CYP1A1* and *CYP1B1* genes and the bone mineral density and serum lipid profiles in postmenopausal Japanese women taking hormone therapy

Jinhua Quan, PhD, Tetsuro Yahata, MD, PhD, Nozomi Tamura, MD, PhD, Hiroshi Nagata, MD, PhD, and Kenichi Tanaka, MD, PhD

Abstract

Objective: The genetic variations of the genes encoding cytochrome P-450 enzymes are considered to play an important role in the metabolism of estradiol. The objective of this study was to evaluate the relationships among single nucleotide polymorphisms (SNPs) of cytochrome P-450 genes, lumbar bone mineral density (BMD), and serum lipids and to determine the effects of hormone therapy (HT).

Design: The participants were 124 Japanese women who had been diagnosed with osteopenia or osteoporosis and were taking HT for 12 months. Seven single nucleotide polymorphisms in the *CYP1A1* and *CYP1B1* genes were characterized. Lumbar BMD and the levels of serum lipids were measured before and after HT.

Results: A single nucleotide polymorphism in exon 3 of *CYP1B1* was found to be significantly associated with the effect of HT on BMD and low-density lipoprotein cholesterol both in univariate and multivariate analyses. In the women with the GG genotype of L432V, the responses to HT of BMD and low-density lipoprotein cholesterol markedly decreased. The serum follicle-stimulating hormone level after HT was significantly higher in the women with the GG genotype of L432V.

Conclusions: These results suggest that the L432V polymorphism in the *CYP1B1* gene could therefore be used to predict the effect of HT on lumbar BMD and low-density lipoprotein cholesterol in Japanese women.

Key Words: Single nucleotide polymorphism – *CYP1A1* – *CYP1B1* – Hormone therapy – Bone mineral density – Low-density lipoprotein cholesterol – Follicle-stimulating hormone.

Estrogen plays a significant role in bone and lipid metabolism, and its deficiency after menopause is the main reason for accelerated bone loss and deterioration of the serum lipid profiles, which are preventable by estrogen administration. A number of observational studies have suggested that hormone therapy (HT) reduces the risk of fractures and coronary events in postmenopausal women.[1-4] However, recently published results from randomized clinical trials of HT indicate that this therapy does not slow the progression of coronary atherosclerosis, whereas the reduction in the hip and clinical vertebral fracture rate is significant.[5,6] Our understanding is limited regarding why not all women benefit from such therapy. However, it is still possible that a genetically determined subgroup of the population could benefit from this therapy.

Postmenopausal HT is generally an effective treatment modality to prevent bone loss while also improving the serum lipid profiles; however, individual variations exist.[7-9] Some postmenopausal women respond strongly to HT, whereas approximately 8% who are compliant with this therapy are nonetheless nonresponders.[2] This raises the possibility that some genetic determinants as well as gene-environment interactions might modulate the responses to HT in individual participants.

Individual genetic variability of estradiol metabolism has been described as a significant contributor to the disease susceptibility with variations depending on ethnic background. Among others, the genetic variations of the genes encoding cytochrome P-450 (CYP) enzymes are considered to play an important role in this regard.[10] CYP enzymes play an important role in the production, bioavailability, and degradation of estradiol. A series of polymorphisms and mutations of the CYP enzyme complex have been identified. *CYP1A1* and *CYP1B1* catalyze the hydroxylation of estradiol and several single nucleotide polymorphic sites of those genes have been described.[11,12] Polymorphisms, especially single nucleotide polymorphisms (SNPs) exist in the exon with amino acid changes, thus leading to functionally relevant biochemical consequences that are therefore capable of influencing the responses to HT.

In this study, we attempted to clarify whether SNPs in the exons of the *CYP1A1* and *CYP1B1* genes affected the change in bone mineral density (BMD) and serum lipid profiles in postmenopausal Japanese women during HT.

Received November 4, 2007; revised and accepted April 17, 2008.

From the Division of Obstetrics and Gynecology, Niigata University Medical and Dental Hospital, Niigata, Japan.

Address correspondence to: Tetsuro Yahata, MD, PhD, Division of Obstetrics and Gynecology, Niigata University Medical and Dental Hospital, 1-757 Asahimachi-dori, Niigata 951-8510, Japan. E-mail: yahatat@med.niigata-u.ac.jp

METHODS

Design

The participants were 124 Japanese women, ranging in age from 40 to 64 years (49.8 ± 1.0 y, mean ± SEM) who had been diagnosed with osteopenia or osteoporosis and were willing to take HT for 12 months. The diagnoses of osteopenia and osteoporosis were based on the criteria recommended by the Japanese Society of Bone and Mineral Research: a lumbar BMD (L2-4) of less than 80% and less than 70% in younger adults (20-44 y), respectively. In all cases, more than 6 months had elapsed since the last menstrual period, the serum estradiol level was lower than 20 pg/mL, and the serum follicle-stimulating hormone (FSH) level was more than 50 mIU/mL. The exclusion criteria were a history of metabolic disease (including hyperparathyroidism, previously diagnosed osteoporosis, or nontraumatic vertebral fracture on baseline radiograph), chronic disease (uncontrolled hypo- or hyperthyroidism, liver disease, or unstable cardiac disease), cancer or thromboembolic disease, a history of treatment with glucocorticoids for more than 6 months, current HT use or HT use within the past 3 months, or a metabolic or other endocrine disease that could influence lipid metabolism. None of the women smoked or drank alcohol to excess, and none engaged in regular strenuous exercise. Furthermore, none had a history of illness or medical therapy, apart from HT, that might affect bone turnover or lipid metabolism. The women were not genetically related. HT was administered either in a sequential regimen (50 women) consisting of 0.625 mg conjugated equine estrogens for 24 days (days 1-24) and 5 mg medroxyprogesterone acetate for 10 days (days 15-24) or a continuous regimen (74 women) consisting of 0.625 mg conjugated equine estrogens and 2.5 mg medroxyprogesterone acetate for 28 days, according to the woman's preference.

Measures

Bone densitometry

BMD, expressed as the mass per unit area (g/cm^2), was measured in the anteroposterior plane of the lumber spine (L2-4), using dual-energy x-ray absorptiometry with a QDR-2000 analyzer (Hologic Inc., Waltham, MA); absorptiometries were examined by the same observer. The average coefficients of variation of the phantom measurements of bone mineral content, bone area, and BMD during the study period were 1.1%, 0.7%, and 0.6%, respectively. In addition, in the control women, the coefficient of variation of the in vivo precision of BMD between two measurements (mean interval: 2.6 ± 1.2 y) was 0.9%. There was no scanner drift observed during the study period. BMD change (ΔBMD) was expressed as the percentage of BMD change compared with the pretreatment baseline.

Analysis of lipids

After an overnight fast (a minimum 12-h fast), blood was collected from each woman to estimate the lipids and lipoproteins. We measured the total cholesterol (Determiner L-TCN; Kyowa Medex, Tokyo, Japan) and triglyceride (L-type Wako TG-H; Wako Pure Chemical, Osaka, Japan) concentrations by enzymatic methods, and the high-density lipoprotein cholesterol concentration by a homogeneous method (Determiner L HDL-C, Kyowa Medex) using a Hitachi 7450 automated analyzer. Low-density lipoprotein cholesterol was calculated using Friedewald's equation.

Hormones and assays

The serum hormone levels were evaluated after 12 months of HT. Blood samples were drawn in the morning after an overnight fast. The serum was separated immediately and frozen at −80°C for future analysis. The hormone levels were measured using an electrochemiluminescent immunoassay for estradiol and a chemiluminescent immunoassay for luteinizing hormone (LH) and FSH. The hormone fractions were measured in three different batches, and a laboratory batch was also treated to determine the random effect in all hormone analyses. The sensitivity, expressed as the minimal detectable dose, was 11.0 pg/mL, 0.11 mIU/mL, and 0.06 mIU/mL for estradiol, LH, and FSH, respectively. The intra- and interassay coefficients of variation were 1.63% and

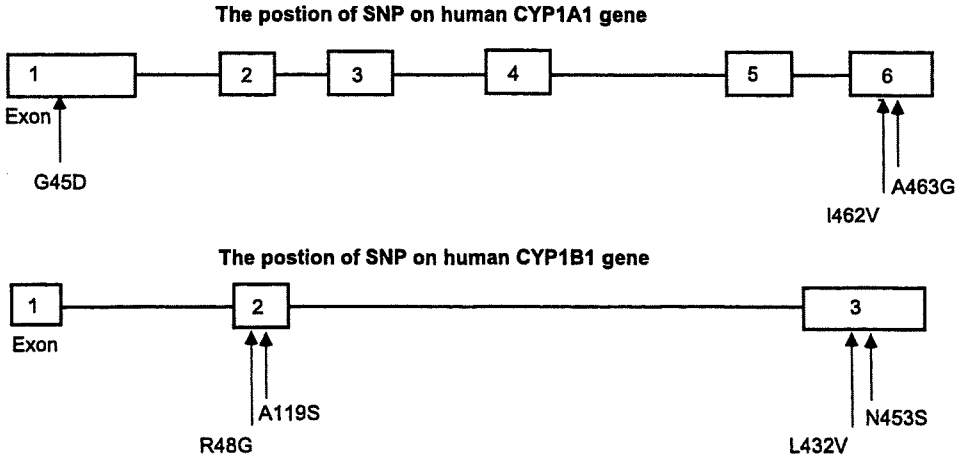

FIG. 1. The position of each single nucleotide polymorphism (SNP) in the *CYP1A1* and *CYP1B1* genes.

TABLE 1. *Genotype and allele frequencies of seven SNPs of CYP gene in Japanese participants*

Gene	Polymorphism	Genotype	Homo (major)	Hetero	Homo (minor)	Allele frequency (major allele) In this study	Sasaki et al	In dbSNP	JSNP ID	dbSNP
CYP1A1	G45D	GA	124 (100%)	0 (0%)	0 (0%)	1.00	—	—	ssj0003953	rs4646422
	I462V	AG	78 (62.9%)	42 (33.9%)	4 (3.2%)	0.80	—	0.902	ssj0007951	rs1048943
	A463G	CG	124 (100%)	0 (0%)	0 (0%)	1.00	—	—	IMS-JST026484	rs2278970
CYP1B1	R48G	CG	90 (72.6%)	16 (12.9%)	18 (1.5%)	0.79	0.68	0.653	ssj0007955	rs10012
	A119S	GT	124 (100%)	0 (0%)	0 (0%)	1.00	0.85	0.648	ssj0007956	rs1056827
	L432V	CG	78 (62.9%)	36 (29.0%)	10 (8.1%)	0.77	0.82	0.592	IMS-JST085313	rs1056836
	N453S	AG	124 (100%)	0 (0%)	0 (0%)	1.00	1.00	0.889	—	rs1800440

SNPs, single nucleotide polymorphisms; CYP, cytochrome P-450; Homo, homozygous; Hetero, heterozygous; JSNP, Japanese Single Nucleotide Polymorphism (database); dbSNP, Single Nucleotide Polymorphism database.

2.24% for estradiol, 3.37% and 3.62% for LH, and 3.50% and 5.28% for FSH.

DNA isolation and genotyping

The peripheral blood samples were collected after informed consent was obtained from each woman. Genomic DNA was extracted from the peripheral blood leukocytes using a DNA purification kit (QIAamp DNA Blood Mini kit; Qiagen, Valencia, CA) according to the manufacturer's instructions. All polymerase chain reactions were performed on a Perkin Elmer GeneAmp 9700 system, and the presence of amplicons was checked on agarose gel. A single nucleotide primer extension assay was performed to analyze SNPs using a SNaPshot Kit (Applied Biosystems, Foster City, CA). The extended primers were analyzed on an ABI 3100 device (Applied Biosystems). The primer sequences for the polymerase chain reactions and primer extension reactions are available in the Japanese Single Nucleotide Polymorphism database. Initial denaturation was performed at 95°C for 2 minutes, followed by 35 cycles each consisting of denaturation at 95°C for 30 seconds, annealing at 60°C, and extension at 72°C for 1 minute, followed by final extension at 72°C for 8 minutes. This study was approved by the Niigata University Human Investigation Committee.

Statistical analysis

Differences in the baseline characteristics, the absolute BMD value, and the serum lipid concentrations among genotypes were tested using an analysis of covariance with age and BMI as covariates. The values of triglycerides were not normally distributed and needed to be log-transformed for the statistical comparisons but, for clarity for presentation, the nontransformed values are presented in the text and tables. To evaluate the relationships between CYP polymorphisms and the change in BMD or serum lipid concentrations during HT, we used repeated-measures analysis of variance. A multiple linear regression model was used to evaluate the simultaneous contributions of different variables. Only those variables that had values of $P < 0.05$ in the univariate analysis were included in the multivariate analyses. All data are expressed as the mean ± SEM. Differences of $P < 0.05$ were considered to indicate statistical significance. All data management and statistical computations were performed with the StatView 4.0 (Abacus Concepts, Berkeley, CA) or the SPSS 10.0 software program (SPSS Inc., Chicago, IL).

RESULTS

In this study, we characterized seven SNPs, three SNPs in the *CYP1A1* gene and four SNPs in the *CYP1B1* gene, from a

TABLE 2. *Baseline characteristics according to the CYP genotypes*

Variables	Genotype of I462V (*CYP1A1*) AA (n = 78)	AG (n = 42)	GG (n = 4)	*P*	Genotype of R48G (*CYP1B1*) CC (n = 90)	CG (n = 16)	GG (n = 18)	*P*	Genotype of L432V (*CYP1B1*) CC (n = 78)	CG (n = 36)	GG (n = 10)	*P*
Age, y	50.1 ± 0.8	49.2 ± 0.8	51.3 ± 1.8	0.73	49.6 ± 0.7	51.5 ± 1.4	49.4 ± 1.2	0.53	50.6 ± 0.8	49.0 ± 0.9	47.8 ± 1.4	0.74
Age at menopause, y	47.4 ± 0.6	47.7 ± 0.6	49.0 ± 1.9	0.89	47.6 ± 0.5	46.3 ± 1.6	48.3 ± 0.5	0.46	47.8 ± 0.6	47.2 ± 0.6	46.6 ± 1.9	0.39
Height, cm	154.9 ± 0.6	151.6 ± 2.4	157.8 ± 7.6	0.19	154.9 ± 0.6	154.9 ± 1.5	153.3 ± 0.9	0.51	153.6 ± 0.9	156.1 ± 1.2	158.5 ± 1.1	0.66
Weight, kg	52.5 ± 0.7	51.7 ± 1.0	51.0 ± 6.0	0.76	51.9 ± 0.7	53.4 ± 1.6	52.5 ± 1.6	0.64	52.0 ± 0.7	52.2 ± 1.2	53.2 ± 2.5	0.40
BMI, kg/m^2	21.9 ± 0.26	25.3 ± 3.5	20.3 ± 0.9	0.38	21.6 ± 0.2	22.3 ± 0.6	22.4 ± 0.6	0.34	23.7 ± 1.9	21.7 ± 0.4	22.1 ± 0.7	0.74
L2-4 BMD, g/cm^3	0.76 ± 0.02	0.76 ± 0.02	0.79 ± 0.08	0.96	0.76 ± 0.02	0.79 ± 0.05	0.75 ± 0.05	0.78	0.77 ± 0.02	0.76 ± 0.02	0.78 ± 0.07	0.23
TC, mg/dL	224.4 ± 4.2	227.2 ± 6.5	231.0 ± 13.5	0.89	223.8 ± 3.9	224.9 ± 8.1	234.5 ± 11.8	0.54	226.2 ± 4.3	228.6 ± 6.8	216.1 ± 10.9	0.65
LDL-C, mg/dL	132.6 ± 4.7	137.3 ± 5.9	132.5 ± 7.2	0.82	130.8 ± 3.8	140.1 ± 0.8	147.3 ± 13.0	0.24	136.1 ± 4.8	135.2 ± 6.2	123.9 ± 10.6	0.60
HDL-C, mg/dL	67.6 ± 1.9	67.0 ± 2.9	77.0 ± 6.8	0.51	67.5 ± 1.8	67.0 ± 2.9	69.6 ± 6.1	0.88	67.4 ± 1.9	68.0 ± 3.1	67.0 ± 6.1	0.98
TGs, mg/dL	122.9 ± 8.8	115.8 ± 11.3	84.8 ± 12.5	0.55	121.2 ± 8.4	114.4 ± 14.3	102.1 ± 11.8	0.60	115.7 ± 9.0	125.3 ± 11.4	125.7 ± 24.5	0.76

CYP, cytochrome P-450; BMI, bone mass index; BMD, bone mineral density; TC, total cholesterol; LDL-C, low-density lipoprotein cholesterol; HDL-C, high-density lipoprotein cholesterol; TGs, triglycerides.
Data are presented as mean ± SE.